

THE COMPARISON OF BAINITIC TRANSFORMATIONS AND
MECHANICAL PROPERTIES OF 60SiMn5 AND 55Cr3 STEELS

A THESIS SUBMITTED TO
THE GRADUATE SCHOOL OF NATURAL AND APPLIED SCIENCES
OF
MIDDLE EAST TECHNICAL UNIVERSITY

BY

SİMGE BAKIR

IN PARTIAL FULFILLMENT OF THE REQUIREMENTS
FOR
THE DEGREE OF MASTER OF SCIENCE
IN
METALLURGICAL AND MATERIALS ENGINEERING

SEPTEMBER 2019

Approval of the thesis:

**THE COMPARISON OF BAINITIC TRANSFORMATIONS AND
MECHANICAL PROPERTIES OF 60SIMN5 AND 55CR3 STEELS**

submitted by **SİMGE BAKIR** in partial fulfillment of the requirements for the degree
of **MASTER OF SCIENCE in METALLURGICAL AND MATERIALS
ENGINEERING Department, Middle East Technical University** by,

Prof. Dr. Halil Kalıpçılar
Dean, Graduate School of **Natural and Applied Sciences**

Prof. Dr. Cemil Hakan Gür
Head of Department, **Met. and Mat. Eng.**

Prof. Dr. Bilgehan Ögel
Supervisor, **Met. and Mat. Eng., METU**

Prof. Dr. Rıza Gürbüz
Co-Supervisor, **Met. and Mat. Eng., METU**

Examining Committee Members:

Prof. Dr. Ali Kalkanlı
Met. and Mat. Eng., METU

Prof. Dr. Bilgehan Ögel
Met. and Mat. Eng., METU

Assist. Prof. Dr. Batur Ercan
Met. and Mat. Eng., METU

Assist. Prof. Dr. Bilge İmer
Met. and Mat. Eng., METU

Prof. Dr. Nuri Durlu
Mech Eng., TOBB Uni. Of Eco. And Tech.

Date: 06.09.2019

I hereby declare that all information in this document has been obtained and presented in accordance with academic rules and ethical conduct. I also declare that, as required by these rules and conduct, I have fully cited and referenced all material and results that are not original to this work.

Name, Surname: SİMGE BAKIR

Signature:

ABSTRACT

THE COMPARISON OF BAINITIC TRANSFORMATIONS AND MECHANICAL PROPERTIES OF 60SiMn5 AND 55Cr3 STEELS

BAKIR, SİMGE

MASTER OF SCIENCE, METALLURGICAL AND MATERIALS
ENGINEERING

Supervisor: Prof. Dr. Bilgehan Ögel
Co-Supervisor: Prof. Dr. Rıza Gürbüz

September 2019, 63 pages

In this study, lower bainitic and martensitic transformations in 55Cr3 and 60SiMn5 heavy duty spring steels were studied. 55Cr3 and 60SiMn5 steels are used in the production of springs that can withstand medium and high tensile and compression loads, especially as leaf springs, helical springs and ring springs in vehicles. A high elastic deformation behavior is expected in spring steels. Therefore, it is important that the spring steel has high yield strength. The transformation mechanisms and mechanical properties of lower bainite were compared with the tempered martensite of 55Cr3. The samples of both steels were austenitized at 860°C for 30 minutes. It was followed by isothermal treatment of 55Cr3 samples at just above M_s temperature, which is 270°C, for 80 minutes in order to obtain fully lower bainitic microstructure. Additionally, incomplete bainitic transformations at either 270°C for 8 minutes or at 270°C for 3 hours were also studied. Moreover, martensitic samples of 55Cr3 were tempered in the range 220°C-550°C. Another set of samples were also treated under M_s in order to obtain mixture of lower bainite and tempered martensite. Although the tempered martensitic samples yielded good impact toughness values, their tensile properties were lower than the lower bainitic samples of 55Cr3. It was seen from the results that the lower bainitic sample of 55Cr3 (270°C, 80min) had 583HV hardness,

1645MPa yield strength, 1978MPa ultimate tensile strength, 9.7% elongation and 12,7J impact toughness values. Moreover, the carbide-free lower bainite of 60SiMn5 was seen to have 600HV, 1781MPa yield strength, 2107MPa ultimate tensile strength, 5,68% elongation and 9J impact toughness values.

Keywords: Lower bainite, carbide-free lower bainite, 55Cr3, 60SiMn5, tempered martensite

ÖZ

60SİMN5 VE 55CR3 ÇELİKLERİNDE BEYİNİTİK DÖNÜŞÜMLERİN VE MEKANİK ÖZELLİKLERİN KARŞILAŞTIRILMASI

BAKIR, SİMGE

Yüksek Lisans, Metalurji ve Malzeme Mühendisliği

Tez Danışmanı: Prof. Dr. Bilgehan Ögel

Ortak Tez Danışmanı: Prof. Dr. Rıza Gürbüz

Eylül 2019, 63 sayfa

Bu tez çalışmasında, 55Cr3 ve 60SiMn5 yay çeliklerinde alt beynitik ve martensitik dönüşümler incelenmiştir. 55Cr3 ve 60SiMn5 çelikleri, özellikle taşıtlarda yaprak yay, helis yay ve bilezik yay olmak üzere, orta ve yüksek şiddette çekme ve basma yüklerine dayanabilen yayların üretiminde kullanılmaktadır. Yay çeliklerinde, yüksek seviyede elastik şekil değiştirme davranışı beklenmektedir. Bu nedenle yay çeliğinin yüksek akma mukavemetine sahip olması önem taşımaktadır. Öncelikle 55Cr3'e ait alt beynit ve temperli martensitin dönüşüm mekanizmaları ve mekanik özellikleri karşılaştırılmıştır. Her iki çeliğe ait numuneler 860°C'de 30dakika boyunca östenitlenmiştir. Ardından, alt beynitik mikroyapı dönüşümünün tamamlanması için, 55Cr3 numuneler martensit oluşum sıcaklığı (M_s) olan 270°C'nin hemen üzerinde, 80 dakika boyunca izotermal ısıtılma tabii tutulmuştur. Bunun yanı sıra, numuneler beynitik dönüşümün başlangıcını gözlemlemek üzere 270°C'de 8 dakika boyunca ve temperlenmiş alt beynitik mikroyapı ve özelliklerini gözlemlemek amacıyla 270°C'de 3 saat boyunca ısıtılma alınmıştır. 220°C'de 5 saat, 450 ° C'de 1.5 saat, 500 ° C'de 1.5 saat, ve 550 ° C'de 1.5 saat temperlenen martensitik numuneler de mekanik testlere alınarak beynitik numunelerle karşılaştırılmıştır. Temperli martensitik numunelerin darbe tokluğu değerleri oldukça iyi sonuçlar verirken (20J), mukavemet açısından alt

beynite göre daha düşük sonuçlar vermiştir. Mekanik teslere göre, 55Cr3 alt bey nitik numunenin (270 ° C, 80 dakika) sertliğinin 583HV, akma mukavemetinin 1645MPa, çekme mukavemetinin 1978MPa, uzama değerinin %9.7 ve darbe tokluğunun 12,7J olduğu görülmüştür. Ayrıca, uygulanan testler sonucu 60SiMn5'in karbür içermeyen alt bey nit numunesinde sertlik değerinin 600HV, akma dayanımının 1781MPa, çekme dayanımının 2107MPa, uzama değerinin % 5,68 ve darbe tokluğunun ise 9J olduğu görülmüştür.

Anahtar Kelimeler: Alt bey nit, karbürsüz alt bey nit, 55Cr3, 60SiMn5, menevişlenmiş martensite

To my precious family

ACKNOWLEDGEMENTS

I would like to express my sincerest gratitude and thanks to my supervisor Prof. Dr. Bilgehan Ögel for guiding and supporting me over the years. He has set a role model of excellence as a researcher, mentor, and instructor. He has provided insightful discussions, advised many times and led me with his knowledge about the research study. He has given me a hand and lightened my way whenever I felt down through all this time. Without his guidance and persistent help, this thesis would not have been possible.

I would also like to express my gratitude to my co-advisor Prof. Dr. Rıza Gürbüz for supporting me through this study.

I would like to thank my thesis committee members for all of their guidance through this process; the discussions, ideas, and feedbacks have been absolutely invaluable.

Special thanks to Asil Çelik Sanayi ve Ticaret A.Ş. for providing the 55Cr3 and 60SiMn5 steel bars. I completed all my study without any trouble in materials supply.

I would like to express my sincere thanks to Cemal Yanardağ and Atalay Özdemir from METU Metallurgical and Materials Engineering Machine Shop for helping me anytime I need support. I would also like to express my gratefulness to Serkan Yılmaz, Zeynep Öztürk, Okan Poyraz and Ecenaz Yurtseven for their great supports during my experiments and analysis. I must also thank to all my lab-mates for their great friendships, support and knowledge sharing. The lab “D-211”, where everyone simply feels like home, will always remain in my mind with good memories.

A good support is the most important thing to survive and stay sane in grad school. I must deeply thank to my manager Rıza Karadaş for always being indulgent and supportive all the time. His friendly manner and mentoring have helped me feel

comfortable whenever I got stuck in this challenging period. I also thank to my colleagues Duygu Bayraktar, Merve Demirlek, Zeynep Bölükoğlu, and Tuğba Aydın from GE Aviation for supporting me through all this period. I must express my special thanks to my friend Volkan Kahyaoğlu for always solving my computer-based inabilities. I am lucky and grateful to be a part of this team.

I must also express my deepest thanks to my closest friends Özgür Polat, Sena Okay, Elif Uğurlu and Seval Dönmez. These four have always been with me at my worst and best times without questioning. Additionally, I would like to thank my dear friends; İrem Çelik, Pınar Tutucu and Ebru Sağ, with whom I shared my childhood and have many great memories. Life would be unbearable without their priceless friendships.

I owe my deepest gratitude to my dear Ufuk Bozkaya for encouraging me during the last and the hardest phase of this work. His surprising and precious existence in my life eased the unbearable times of this period. I thank to the universe for letting us meet somewhere on the Earth.

Finally, deeply from my heart, I would like to thank and dedicate this thesis to my precious family. I am and will always be grateful to my mother; Fethiye Doğan for showing me the value of achievement of hard work with unconditional love and care; to my father Ali Rıza Bakır for always preaching me the importance of reading and research. My greatest gratitude is to my precious sister Sibel Boztaş and my beloved brother Sinan Bakır, whom have been my best friends and second parents all my life. They have always inspired me with their success and great perspective. I also would like to thank my brother in law Ömer Boztaş for assisting me through my thesis journey with his invaluable inputs. I must express my deepest love to my precious nephew Ozi for showing me the miracles of life and fascinating me with his cuteness. My trips to Ankara would have not been so excited and meaningful without you, Ozim!

I am the luckiest to have you. I love you all dearly!

TABLE OF CONTENTS

ABSTRACT	v
ÖZ	vii
ACKNOWLEDGEMENTS.....	x
TABLE OF CONTENTS	xii
LIST OF TABLES.....	xiv
LIST OF FIGURES	xv
LIST OF ABBREVIATIONS.....	xix
1. INTRODUCTION.....	1
2. LITERATURE REVIEW AND THEORY	3
2.1. Martensite.....	3
2.1.1. Tempered Martensite.....	6
2.2. Bainite	7
2.2.1. Upper Bainite	10
2.2.2. Lower Bainite	10
3. EXPERIMENTAL SETUP AND PROCEDURE.....	13
3.1. Materials.....	13
3.2. Heat Treatment Equipment	14
3.3. Heat Treatment Processes	14
3.4. Microstructural Examination	15
3.5. Mechanical Tests.....	15
3.5.1. Fractography.....	17
4. EXPERIMENTAL Results.....	19

4.1. Isothermal Transformation (TTT) Data.....	19
4.2. Heat Treatment of 55Cr3.....	21
4.3. Heat Treatment of 60SiMn5.....	24
4.4. Microstructural Examinations	24
4.4.1. Microstructural Examinations for 55Cr3.....	25
4.4.1.1. Martensitic Transformation in 55Cr3.....	25
4.4.1.2. Lower Bainitic Transformation.....	28
4.4.1.3. Isothermal Transformations Below M_s Temperature.....	31
4.4.2. Phase Transformations in 60SiMn5.....	32
4.4.2.1. Lower Bainitic Transformation.....	33
4.4.3. Comparison of Lower Bainitic Microstructures of 55Cr3 and 60SiMn5 under SEM.....	34
4.5. Mechanical Test Results.....	38
4.5.1. Hardness Tests	38
4.5.2. Tensile Tests	39
4.5.3. Charpy Impact Test Results.....	43
5. DISCUSSION.....	49
5.1. Microstructural Characterization of 55Cr3 and 60SiMn5.....	49
5.2. Comparison of Mechanical Properties of 55Cr3 and 60SiMn5 Samples.....	51
6. CONCLUSION.....	59
REFERENCES.....	61
CURRICULUM VITAE	65

LIST OF TABLES

TABLES

Table 2.1 Stored free energies of a variety of microstructures [7] [8]	7
Table 3.1. Chemical compositions of 55Cr3 and 60SiMn5 conforming to EN 10089	13
Table 3.2. Corresponding notations of 55Cr3 and 60SiMn5 in different norms.....	13
Table 4.1. Lower bainite transformation data for 55Cr3 and 60SiMn5	20
Table 4.2. Heat treatment routes for 55Cr3	23
Table 4.3. Heat treatment route for 60SiMn5.....	24
Table 4.4. Hardness test results for 55Cr3 and 60SiMn5 samples	38
Table 4.5. Tensile test results for 55Cr3 & 60SiMn5 samples.....	40
Table 4.6. Charpy impact test results for 55Cr3 and 60SiMn5 samples	44

LIST OF FIGURES

FIGURES

Figure 2.1. Microstructure of a plate martensite in an Fe-1.86%C alloy [5]	3
Figure 2.2. Displacement of iron atoms (open circles) by carbon atoms (black circles) in tetragonal unit cell of martensite [5]	4
Figure 2.3. M_s temperatures and morphologies of martensite as a function of carbon content superimposed on the iron-carbon equilibrium diagram [6].....	5
Figure 2.4. Optical micrographs of (a) Lath martensite in 4130 steel quenched to martensite and tempered at 150°C and (b) plate martensite in the high-carbon case of a carburized steel. The martensite plates etch dark, white regions are retained austenite [26].	6
Figure 2.5. The shapes of pearlite and bainite during growth. The edgewise growth of bainite is governed by the growth of Widmanstaetten ferrite [11]	8
Figure 2.6. Microstructural differences between pearlite and bainite through isothermal transformation of austenite [10]	8
Figure 2.7. Visibility of bainite nose with the addition of Mn [22]	9
Figure 2.8. Effect of alloying elements on TTT diagram [14].....	10
Figure 2.9. SEM micrographs of low-carbon bainitic steels isothermally treated at 350°C for 3600s; (a) base, (b) Cr addition	11
Figure 3.1. (a) Muffle furnace and (b) salt bath used for austenitization and isothermal heat treatment	14
Figure 3.2. Cross-sectional cut-ups for microstructural examination	15
Figure 3.3. Tensile test specimen machined from 55Cr3 according to ASTM E8/E8M-16a.....	16
Figure 3.4. Charpy impact test specimen machined from 55Cr3 according to ASTM E23-16b	16
Figure 4.1. TTT diagram generated by JmatPro® for 55Cr3	19

Figure 4.2. TTT diagram generated by JmatPro® for 55Cr3	20
Figure 4.3. Routes for tempered martensitic microstructures of 55Cr3	21
Figure 4.4. Routes for lower bainitic microstructures of 55Cr3	22
Figure 4.5. Route for under M ₅₀ treatment for 55Cr3 steel	23
Figure 4.6. Route for lower bainite transformation of 60SiMn5	24
Figure 4.7. As-quenched martensite	25
Figure 4.8. The optical micrograph of tempered martensite. (220°C, 5hrs)	26
Figure 4.9. The optical micrograph of tempered martensite. (450°C, 1,5hr).....	26
Figure 4.10. The optical micrograph of tempered martensite. (500°C, 1,5hr).....	27
Figure 4.11. The optical micrograph of tempered martensite. (550°C, 1,5hrs).....	27
Figure 4.12. Isothermally treated (270°C, 8min). Lower bainite needles (dark) together with martensite phase (white matrix).	28
Figure 4.13. Optical micrograph of isothermally treated specimen at 270°C for 8 min	29
Figure 4.14. Optical micrograph of isothermally treated specimen at 270°C for 80 min. Bainite transformation is completed.	29
Figure 4.15. Optical micrograph of isothermally held sample at 270°C for 80 min.	30
Figure 4.16. Optical micrograph of isothermally held sample at 270°C for 3 hrs.....	30
Figure 4.17. Optical micrograph of isothermally held sample at 270°C for 3 hrs.....	31
Figure 4.18. Optical micrograph of isothermally treated sample at M ₅₀ 270°C for 3 hrs	32
Figure 4.19. Optical micrograph of isothermally treated sample at M ₅₀ 270°C for 3 hrs	32
Figure 4.20. The route for lower bainitic microstructure of 60SiMn5	33
Figure 4.21. Optical micrograph of isothermally held sample at 250°C for 5,5hrs... ..	33
Figure 4.22. Optical micrograph of isothermally held sample at 250°C for 5,5 hrs.. ..	34
Figure 4.23. SEM micrographs of (a) 55Cr3 lower bainite, 270°C 80min, (b) 60SiMn5 lower bainite, 250°C 5,5hr	35

Figure 4.24. SEM micrographs of (a) & (c) 55Cr3 lower bainite with carbides (270°C 80min), (b) & (d) 60SiMn5 lower bainite (250°C 5,5hr). Carbides are seen in 55Cr3, whereas no carbides are seen in 60SiMn5 specimen	37
Figure 4.25. Hardness values of 55Cr3 samples after application of various heat treatment routes.....	39
Figure 4.26. Fracture surfaces of the tensile test specimens quenched and tempered at 220°C, 5hr.	41
Figure 4.27. Fracture surfaces of the tensile test specimens quenched and tempered at 450°C, 1.5hr.	41
Figure 4.28. Fracture surfaces of the tensile test specimens of lower bainite transformed 270°C, 80min.	42
Figure 4.29. Fracture surfaces of the tensile test specimens of under M _s treatment at 240°C, 5hr.	42
Figure 4.30. Fracture surfaces of the tensile test specimens of lower bainite transformed at 250°C, 5,5hr.	43
Figure 4.31. Graph for impact energy values of 55Cr3 and 60SiMn5 samples.....	44
Figure 4.32. Fracture surfaces of Charpy impact test specimens of tempered martensite at 450°C, 1,5hr.....	45
Figure 4.33. Fracture surfaces of Charpy impact test specimens of tempered martensite at 220°C, 5hr.....	45
Figure 4.34. Fracture surfaces of Charpy impact test specimens of lower bainite transformed at 270°C, 80min.	46
Figure 4.35. Fracture surfaces of Charpy impact test specimens of lower bainite transformed at 270°C, 80min (higher magnification).	46
Figure 4.36. Fracture surfaces of Charpy impact test specimens of under M _s treatment at 240°C, 5hr.....	47
Figure 4.37. Fracture surfaces of Charpy impact test specimens of carbide-free lower bainite of 60SiMn5 Mn5 transformed at 250°C, 5,5hr.....	47
Figure 4.38. Fracture surfaces of Charpy impact test specimens of carbide-free lower bainite of 60SiMn5 transformed at 250°C, 5,5hr. (higher magnification).	48

Figure 5.1. TEM micrographs of (a) lower bainite and (b) tempered martensite of JIS SK5 steel [37]	50
Figure 5.2. Cr-free and Cr-added steels austempered at 400°C; (a,c) Cr-free steel; (b,d) Cr-added steel. M, martensite; BF, bainitic ferrite; RA, retained austenite.[15].....	53
Figure 5.3. Comparison of the tensile properties of 55Cr3 LB and 60SiMn5 CFLB	57
Figure 5.4. Charpy Impact Energy vs. Tensile Strength of lower bainitic microstructures of 55Cr3 and 60SiMn5	57

LIST OF ABBREVIATIONS

ABBREVIATIONS

TTT - Time – Temperature – Transformation

IT - Isothermal Transformation

LB - Lower Bainite

CFLB - Carbide-free Lower Bainite

TM - Tempered Bainite

FM - Fresh Martensite

WQ - Water Quench

OQ - Oil Quench

UTS - Ultimate Tensile Strength

ASTM - American Society of Testing Materials

Q&T - Quenched and Tempered

M_s - Martensite Start Temperature

M_f - Martensite Finish Temperature

T_B - Bainite Transformation Temperature

B_s - Bainite Start

B_f - Bainite Finish

T_t - Tempering Temperature

CHAPTER 1

INTRODUCTION

Martensitic steels offer the best combination of strength, toughness and fatigue resistance. However, at high strength values martensite is very brittle.

An important and a historical attempt came from Bain and Davenport during the late 1920s. They studied isothermal transformation techniques of austenite within the temperature range just above martensite start and below fine pearlite formation. They discovered a new microstructure consisting of an “acicular, dark etching aggregate” unlike to pearlite and martensite.

With the discovery of this new microstructure, Bain stated that they reached a property tougher than the tempered martensite with the same hardness [1]. This exploration would create a big influence in industry since it would eliminate the need for additional heat treatments as in tempering the martensite. However, the long transformation times needed for bainite formation limited the industrial applications.

The pressure on automotive industry for safer, more energy efficient and environmentally friendly cars lead to the replacement of mild steels with high-strength steels at an increasing trend. [29]. In recent years many commercial low carbon bainitic steels become available in the market. These include creep resistant steels [30, 31], bainitic forging steels [32, 33] and complex phase (CP) steels with bainitic constituents [34, 35].

Bainite transformation occurs by growth of bainitic ferrite sheaves into the austenite grains in a displacive mechanism that carbon is partitioned between ferrite and austenite. As the solubility of carbon in ferrite is very low, it precipitates within the bainite sheaves in the form of fine cementite. However, the precipitated cementite may act as crack initiation site and may limit the toughness of bainite.

In recent years, Bhadeshia and Caballero has developed a series of carbide free bainitic steels containing high C and high Si with an ultimate tensile strength in the range 2.0 GPa and a toughness of as high as 30MPa.m^{1/2} [16]. The presence of high %Si suppresses the carbide precipitation within bainite sheaves (bainitic ferrite).

In this study the effect of martensitic and bainitic microstructures on mechanical properties of low alloy steels 55Cr3 and 60SiMn5 are studied. For this purpose, the spring steel 55Cr3 is selected for investigation and different heat treatment procedures are applied to obtain 100% bainitic, 100% martensitic or martensitic-bainitic phase mixtures to observe the effects on mechanical properties. Therefore, it would be possible to study the behavior of a hard phase (martensite) present in a relatively tough phase (bainite). On the other hand, 60SiMn5 spring steel is a high Si steel. Si retards the cementite precipitation in bainite. On the other hand, Cr is a carbide forming element. Therefore, it would be a good opportunity to compare the properties of bainite in 55Cr3 steel and 60SiMn5 steel.

CHAPTER 2

LITERATURE REVIEW AND THEORY

The purpose of this chapter is to review the literature on martensitic and bainitic microstructures of steels, differences of the transformation mechanisms of these microstructures, the effects of alloying elements on TTT diagram, final microstructures and mechanical properties.

2.1. Martensite

Austenite decomposes to different equilibrium structures when cooled by different cooling rates. On the other hand, when it is cooled with such a high rate that it results in a non-equilibrium condition, an alternative transformation occurs. Due to this rapid cooling, a non-equilibrium metastable phase called “martensite”, which is a supersaturated solid solution of carbon in ferrite, is formed, which comprises of lath-like needles on austenite matrix as can be seen in Figure 2.1 [4]. Since it is not an equilibrium phase, martensite cannot be seen on iron carbon equilibrium phase diagram. It can be seen on time-temperature-transformation diagrams of steels.

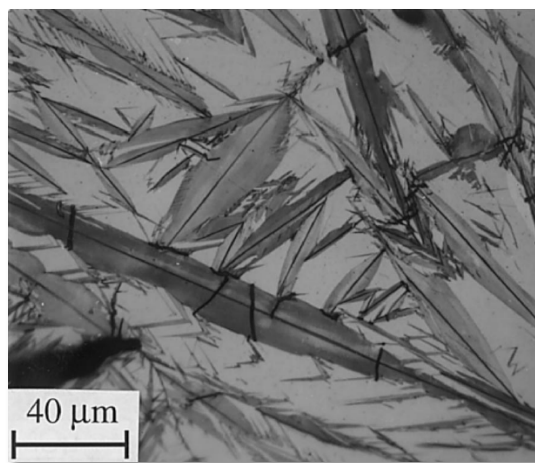


Figure 2.1. Microstructure of a plate martensite in an Fe-1.86%C alloy [5]

The martensite formation and completion temperatures are defined as M_s and M_f on TTT diagrams, respectively. In order to obtain martensite, the cooling rate needs to be adjusted such that the pearlite and bainite noses on TTT shall not be crossed. Moreover, for a fully martensitic structure, M_f should be passed. If M_f is below room temperature, then there will be retained austenite in the resulting microstructure even if M_f is achieved.

In the crystal structure of martensite, the carbon atoms create substantial strains or displacements of the nearest neighbor iron atoms. Figure 2.2 shows a schematic diagram of the iron atom displacements due to the carbon atoms. Thus, if carbon atom diffusion is suppressed by quenching, they are trapped in the set of octahedral sites which produce the tetragonality of the martensitic structure called as “body centered tetragonal”, and await the arrival of the dislocations set in motion by the generation of critical resolved shear stresses during mechanical testing.

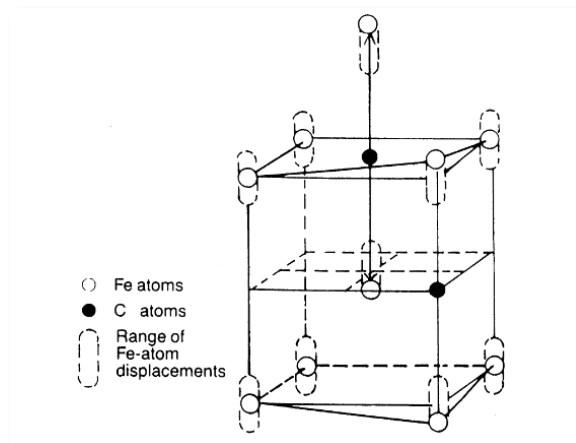


Figure 2.2. Displacement of iron atoms (open circles) by carbon atoms (black circles) in tetragonal unit cell of martensite [5]

The increasing interactions of the strain fields of moving dislocations with the increasing lattice strains due to the carbon atoms creates the strong dependency of the strength of martensite on carbon [5].

In their study, Kraus et al. [6] explained how M_s temperatures and martensite morphologies change as a function of carbon content. Figure 2.3 illustrates that the M_s temperature decreases as the carbon content increases. The decrease in M_s influences two phenomena relative to tempering. Firstly, the high M_s temperatures of low carbon steels and the accompanied large range of cooling to room temperature, sometimes causes microstructural changes and carbon rearrangement to occur during quenching or cooling prior to applied tempering heat treatments.

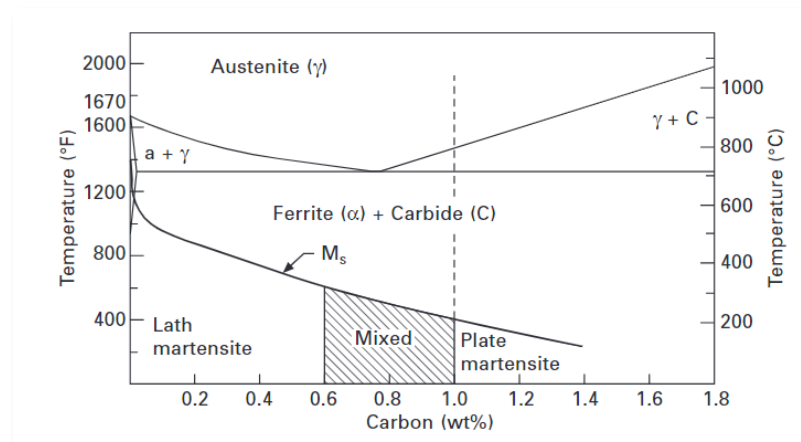


Figure 2.3. M_s temperatures and morphologies of martensite as a function of carbon content superimposed on the iron-carbon equilibrium diagram [6]

Secondly, the possibility of retained austenite to exist in the final microstructure and the restriction of diffusional changes to occur during quenching may increase due to the low M_s temperatures of steels with higher carbon content. Figure 2.3 also shows the morphology changes with respect to carbon content and M_s temperature. In support, the differences in morphologies of martensite are illustrated in Figure 2.5. The “lath”, in other words, board-shaped martensite forms in low and medium carbon steels; whereas plate-shaped martensite forms in high carbon steels. Contrary to plate martensite, lath martensite is very fine having the width thinner than 0.5 micron [26].

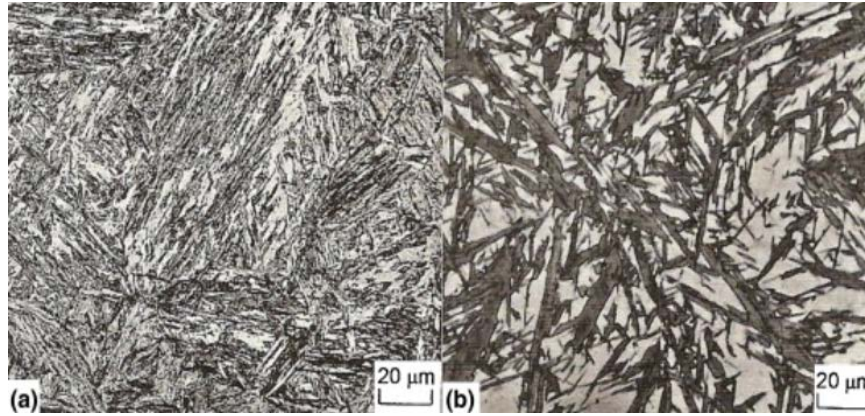


Figure 2.4. Optical micrographs of (a) Lath martensite in 4130 steel quenched to martensite and tempered at 150°C and (b) plate martensite in the high-carbon case of a carburized steel. The martensite plates etch dark, white regions are retained austenite [26].

2.1.1. Tempered Martensite

In the hardened, in other words as-quenched condition of steel, fully martensitic microstructure should be obtained in order to have maximum yield strength. On the other hand, although its high yield strength, martensitic structure is very brittle. Hence, as-quenched steels are used for very few engineering applications. Therefore, in order to overcome this negative aspect of martensite, tempering process is applied so that the properties of quenched steels are modified to increase ductility without sacrificing from the strength [24].

Bhadeshia and Honeycombe (2017) pointed out that the inclination of the microstructure to respond to a tempering heat treatment depends on how far it diverts from equilibrium. In the same vein, Bhadeshia and Strang (2013) supported this statement by outlining that the highest stored energy increment originates from the entrapment of carbon in supersaturated ferrite. Assuming the stored energy of ferrite, graphite and cementite as zero, in Table 2.1 martensite has the highest stored energy and differentiates from supersaturated ferrite by its strain and interfacial energies which are due to the formation mechanism of martensite [7] [8].

Table 2.1 *Stored free energies of a variety of microstructures [7] [8]*

Phase mixture in Fe-0.2C-1.5Mn wt% at 300K	Stored energy/J mol ⁻¹
Ferrite, graphite and cementite	0
Ferrite and cementite	70
Para-equilibrium ferrite and para-equilibrium cementite	385
Supersaturated ferrite	1214
Martensite	1914

Although martensite has high tensile strength among the other microstructures most of the time, this highly stored energy in martensite during its transformation causes internal stresses which cause negative effects on material. When exposed to stress, it always shows brittle behavior in as-quenched condition. Therefore, in order to improve its mechanical properties, tempering is applied thereby relieve the stresses stuck in the microstructure. Hence the brittleness decreases and the ductility increases.

Tempering heat treatment is applied to the steels to relieve the stresses entrapped in the microstructure due to quenching or deformations. The tempering temperature shall be chosen at such a temperature that the steel does not undergo temper embrittlement. The temper embrittlement is tempering the steel at a temperature and for a time that the impurity elements in the steel segregate at the prior austenite grain boundaries which in turn cause negative effects on mechanical properties [9].

Although the phases after tempering are ferrite and cementite, the microstructure is referred as tempered martensite as it originates from martensitic microstructure and keeps some morphological characteristics of martensite. The changes in microstructure are strongly affected by carbon content and alloying elements since these affect the composition of carbide that form and precipitate during tempering [7].

2.2. Bainite

Bainite is a phase mixture formed by high rate of cooling of austenite. Likely to martensite, bainite is also a non-equilibrium phase; therefore, cannot be seen on iron-carbon equilibrium phase diagram. The morphology of martensite and bainite are very likely to each other. But their formation mechanisms are completely different than

each other. Unlike martensite, bainite formation is diffusion dependent and associated with carbide precipitation and a lower dislocation density [10].

When looking at their morphologies, bainite and pearlite may look very similar. However, this was refuted by Hillert et al. by having demonstrated that a pearlite colony comprise of a combined structure of ferrite and cementite which grow cooperatively as in Figure 2.4. In the bainite, on the other hand, the plates of bainitic ferrite forms first and cementite precipitation occurs subsequently [10,11].

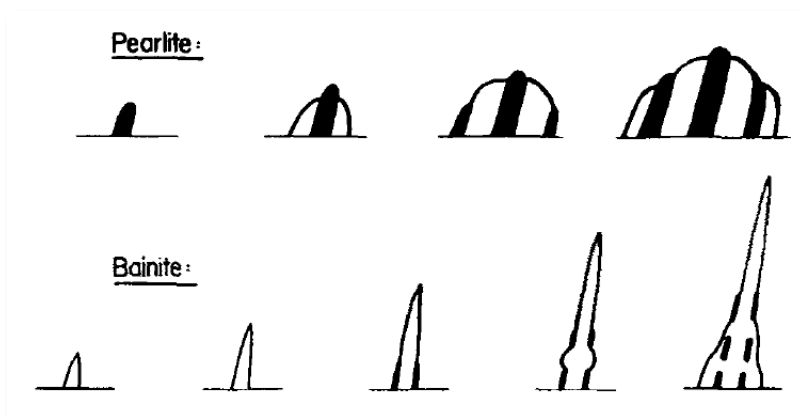


Figure 2.5. The shapes of pearlite and bainite during growth. The edgewise growth of bainite is governed by the growth of Widmanstaetten ferrite [11]

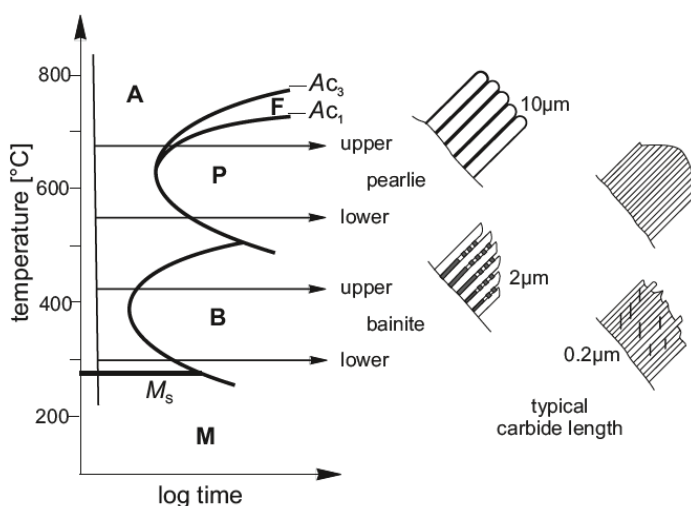


Figure 2.6. Microstructural differences between pearlite and bainite through isothermal transformation of austenite [10]

Bainite forms by quenching austenite to a temperature region where bainite forms on TTT diagram and keeping it at a certain temperature until the required time for completion is achieved as it can be seen from Figure 2.6.

If the TTT diagrams are more focused, it is clear that all TTT diagrams consist of basically two C-shaped curves. These curves sometimes cannot be differentiated and seem as there is only one curve due to the curves being overlapped. This is the case when the hardenability of the steel decreases. On the other hand, there are TTT curves as illustrated for Fe-0,4C-2Mn wt% in Figure 2.7, where two C-curves are clearly visible. Mn addition brings hardenability and this separates the two curves due to the slower transformation rates [22]. The separation of the bainite and pearlite curves enables to obtain desired final microstructure and mechanical properties more accurately.

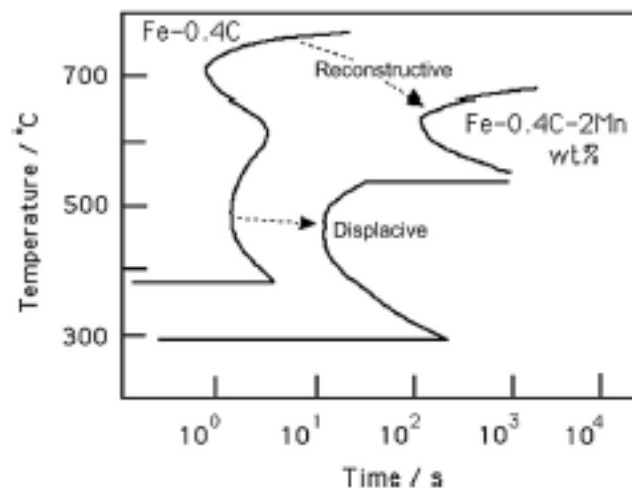


Figure 2.7. Visibility of bainite nose with the addition of Mn [22]

Bainite region on TTT also divides into two regions as upper bainite and lower bainite as illustrated in Figure 2.6. They have differences both in the microstructure and the mechanical properties.

2.2.1. Upper Bainite

The transformation mechanism of austenite to the upper bainite comprises of two steps. The ferrite plates at austenite grain boundaries nucleates and grows in the first step. The growth of these ferrite plates continues until they impinge with other platelets and the driving force for growth reduces due to the rejected carbon into austenite. At the end of the first step, the austenite gets stabilized enough not to transform to martensite and a "fully austempered" structure is obtained. In the second step, together with the thickening of ferrite plates, iron carbides nucleate at the expense of austenite [12].

2.2.2. Lower Bainite

Steels are manipulated by some means to get the most desired final microstructure. In order to get the superior properties of the lower bainitic microstructure than martensite, alloying element addition is done. By the addition of appropriate alloying elements, TTT diagram is shifted to the right and downwards. This means, after the addition of alloying elements, lower bainite formation will be much more attainable since bainite nose becomes more visible and easier to cut and martensite formation is suppressed by lowering M_s temperature.

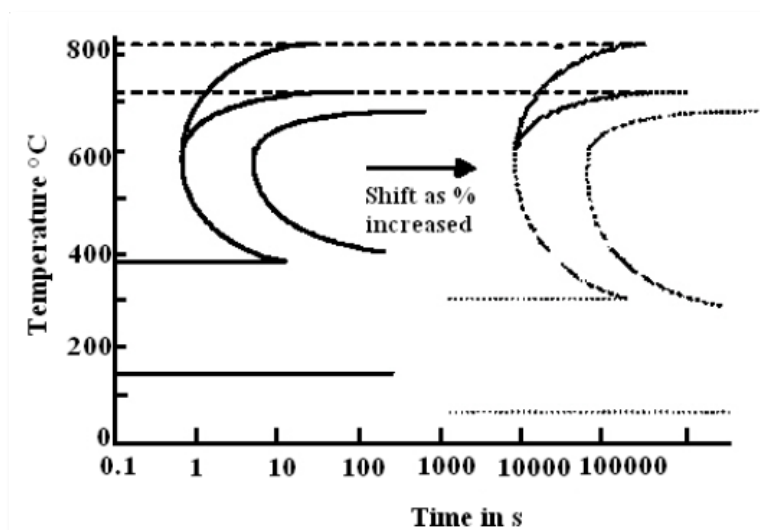


Figure 2.8. Effect of alloying elements on TTT diagram [14]

The key element in the suppression of martensite is carbon. High carbon content causes M_s to decrease and enables bainite formation to occur at lower temperatures. In order to improve the properties of final desired microstructure, other elements like silicon, aluminum, cobalt, manganese, and chromium are added. Silicon is added to suppress cementite precipitation, which acts like a crack initiator and is needed to be avoided especially in high strength steels. Al and Co are good accelerators for the reaction kinetics; therefore, their addition increases the reaction rate. For the hardenability, Mn and Cr is added [13].

In this study, the effects of Cr and Si on phase transformations and on the mechanical properties of the steels are the main area of focus. Therefore, how Cr and Si affect these mechanisms are described specifically.

In their study, Sharma et.al. [24] reported that Cr addition significantly increases bainite amount in the steel. After austenitization, an isothermal treatment was applied at 350°C for 3600 seconds to the specimens. As a result, it was revealed that the specimen with Cr mainly consists of lath-like bainite rather than martensite (Figure 2.9 (b)); whereas, the base steel has much less bainite (Figure 2.9 (a)).

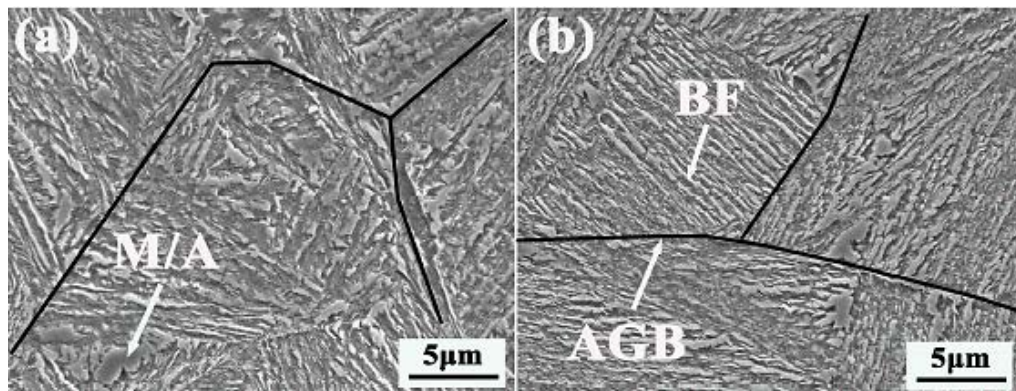


Figure 2.9. SEM micrographs of low-carbon bainitic steels isothermally treated at 350°C for 3600s; (a) base, (b) Cr addition

An exciting contribution to the research area of bainite has come from Sandvik et.al., by the exploration of carbide-free bainite microstructures which have both high toughness and high strength in the 1980s. They were the first to achieve an ultra-fine bainitic structure by holding the high-carbon high-silicon steel isothermally at low temperature. Soliman et.al., reported that the silicon has very low solubility in cementite and very limited mobility at the bainite formation temperature. As a consequence, silicon is entrapped in untransformed austenite during para-equilibrium formation of bainitic ferrite and cementite precipitation is suppressed [27, 28].

CHAPTER 3

EXPERIMENTAL SETUP AND PROCEDURE

This chapter describes the materials and methods used in this study. It covers the materials, the equipment used, and the heat treatment routes applied to the samples. The determination of the methods used for microstructural analysis by optical microscopy and SEM, hardness tests, tensile tests and Charpy impact tests and fractography evaluation are also described.

3.1. Materials

In this study, 55Cr3 and 60SiMn5 steels were used. These steels are in spring steels category and supplied from Asil Çelik Sanayi ve Ticaret A.Ş. Table 3.1 shows the chemical compositions of 55Cr3 and 60SiMn5. Table 3.2 shows the corresponding notations of 55Cr3 and 60SiMn5 in different standards.

Table 3.1. *Chemical compositions of 55Cr3 and 60SiMn5 conforming to EN 10089*

Steel	Material No.	%C	%Si	%Mn	P Max.	S Max.	%Cr	N Max.
55Cr3	1.7176	0,52- 0.60	Max 0,40	0,70- 1,00	0,025	0,025	0,70- 1,00	-
60SiMn5	1.0908	0,55- 0.65	1,00- 1.30	0,90- 1,10	0,050	0,050	-	0,007

Table 3.2. *Corresponding notations of 55Cr3 and 60SiMn5 in different norms*

Euro Norm/EN		DIN	SAE/AISI	BS	FNOR
Short Notation	Material No.				
55Cr3	1.7176	55Cr3	5155	527A61 (EN48)	55Cr3
60SiMn5	1.0908	60SiMn5	-	-	-

3.2. Heat Treatment Equipment

Austenitization of samples were done in Protherm muffle furnace (Figure 3.1 (a)) and then quenched in Protherm salt bath (Figure 3.1(b)) for bainitic transformation. The salt bath contains AS 135 Tempering Salt (Petrofer), which consists of alkaline nitrates and nitrites with a working temperature range of 160°C to 550°C. The salt bath temperature is controlled within $\pm 5^\circ\text{C}$.

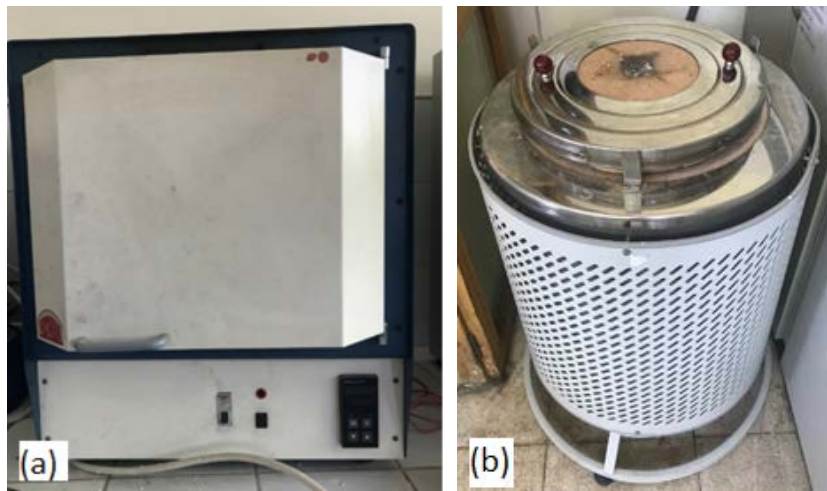


Figure 3.1. (a) Muffle furnace and (b) salt bath used for austenitization and isothermal heat treatment

3.3. Heat Treatment Processes

The TTT diagrams for both 55Cr3 and 60SiMn5 steels were originated by JMatPro[®] software. According to the heat treatments applied, the materials were divided into subgroups. All materials were firstly austenitized at 860°C for 30 minutes. The tempered experiments of 55Cr3 steel were done by holding the specimens at various tempering temperatures and durations followed by oil quenching. The lower bainite experiments of both 55Cr3 and 60SiMn5 steels were done by holding the specimens isothermally just above M_s temperature. After isothermal treatment all the samples are water quenched. In addition, several specimens are heat treated to obtain a mixture of bainitic-martensitic structures.

3.4. Microstructural Examination

In this study, the preliminary heat treatment studies were done by using the specimens with the dimensions of 2cm x 2cm x 2cm from 55Cr3 and 60SiMn5 steels as illustrated in Figure 3.2. After the heat treatments, all specimens were sectioned by Metkon Metacut 251 Abrasive Cutter to get rid of the decarburized layer. Then specimens were mounted by using Metkon Ecompress 100 mounting machine. After grinding with emery papers from coarse to finer, the polishing was applied with 6 μ and 1 μ Metkon Diapat-P water based polycrystalline diamond suspension. Once a smooth surface was achieved, specimens were etched in 2% Nital solution.

For microstructural analysis Huvitz Digital Optical Microscope HDS-5800 and FEI Nova Nanosem 430 Scanning Electron Microscope was used.

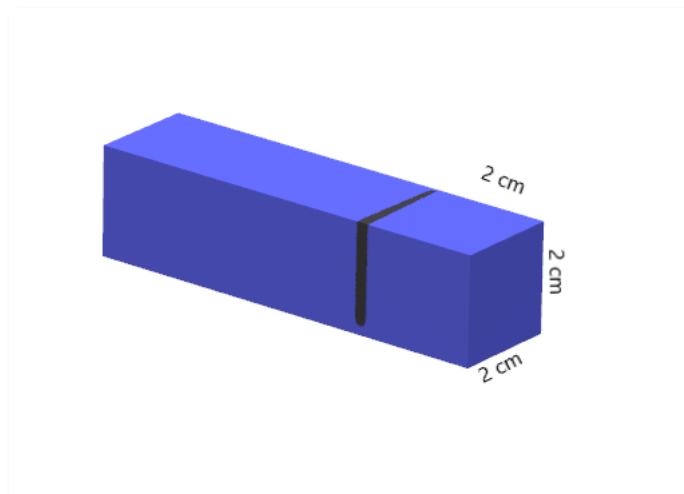


Figure 3.2. Cross-sectional cut-ups for microstructural examination

3.5. Mechanical Tests

The hardness of the specimens was measured by EMCO M4U-025 instrument using Vickers indenter with a load of 30kgf. The tests were done according to ASTM E92-82/E2. The specimen surfaces were in as-polished condition.

Tensile test specimens were machined round as illustrated in Figure 3.3 according to ASTM E8/E8M-16a standard. The dimensions were chosen as 8 mm for gage diameter and 40 mm for length.



Figure 3.3. Tensile test specimen machined from 55Cr3 according to ASTM E8/E8M-16a

For tensile test, INSTRON 5582 Universal Testing Machine was used. In order to collect accurate data, 2 specimens for each heat treatment route were tested and the mean values of the test results were used.

The Charpy impact test specimens were machined as shown in Figure 3.4 according to ASTM E23-16b standard. The dimensions of the specimens were 10mm x 10mm x 55mm and a “V” shape notch was machined perpendicular to the rolling direction of plate.

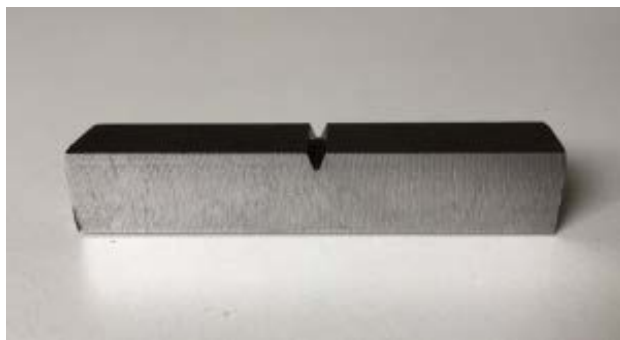


Figure 3.4. Charpy impact test specimen machined from 55Cr3 according to ASTM E23-16b

A pendulum type TINIUS-OLSEN Charpy impact test machine was used for the test. In order to collect accurate data, 3 specimens of each heat treatment route were tested and the mean values of the results were used.

3.5.1. Fractography

After the tensile test and V-notched Charpy impact test, the fracture surfaces were examined under FEI Nova Nanosem 430.

CHAPTER 4

EXPERIMENTAL RESULTS

In this part, the results of the heat treatments applied to 55Cr3 and 60SiMn5 samples are compared by means of microstructure and mechanical properties.

4.1. Isothermal Transformation (TTT) Data

TTT diagrams are the most critical tools to determine the heat treatment routes. The calculated TTT diagrams for 60SiMn5 and 55Cr3 were generated by JmatPro® software and given in Figure 4.1 and Figure 4.2.

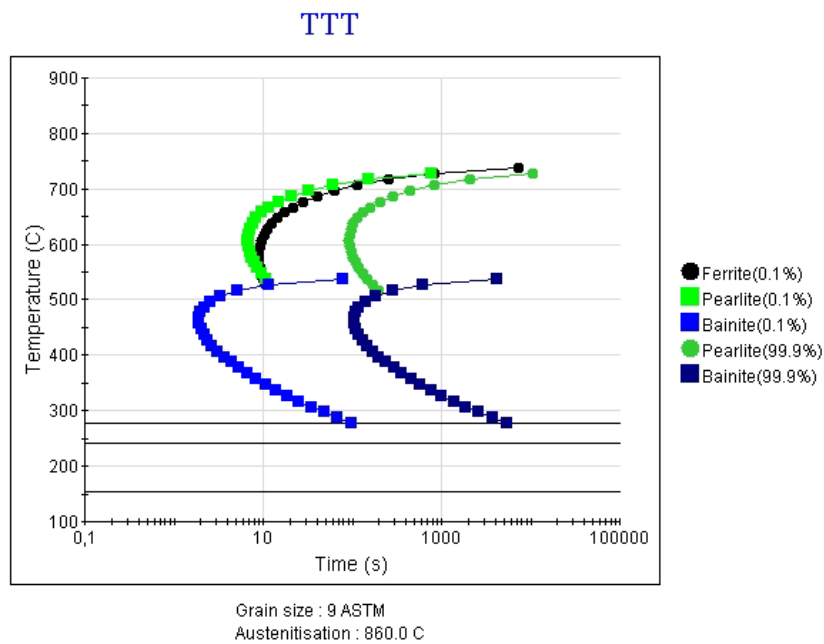


Figure 4.1. TTT diagram generated by JmatPro® for 55Cr3

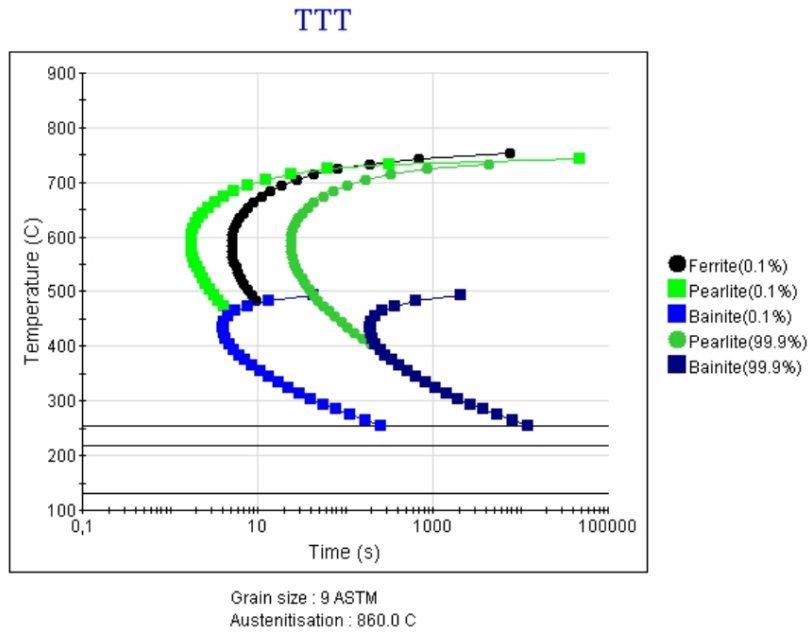


Figure 4.2. TTT diagram generated by JmatPro® for 55Cr3

The strength of the bainite increases with a decrease in transformation temperature. Mateo et.al., related the increase in strength to the amount of carbon that trapped inside the bainitic ferrite and the formation of thinner ferrite sheaves in bainite [23]. Therefore, it can be stated that the strongest bainite will form upon an isothermal transformation at a temperature just above M_s . From Figure 3.2, it is seen that M_s temperatures for 55Cr3 and 60MnSi5 are 270°C and 250°C respectively. On the graphs, the bainite start and bainite finish times were read as 8 minutes and 80 minutes respectively at 270°C for 55Cr3 steel. The same parameters were 5 minutes and 5,5 hours respectively at 250°C for 60SiMn5 steel. The austenitization temperature was selected as 860°C for both steels. As seen in Table 4.1, bainite starts to form in a very short time after quenching to the transformation temperature.

Table 4.1. Lower bainite transformation data for 55Cr3 and 60SiMn5

Steel	M_s (°C)	B_s	B_f
55Cr3	270	8 min	80 min
60SiMn5	250	5 min	5,5 hr

4.2. Heat Treatment of 55Cr3

55Cr3 samples were heat treated to achieve martensitic, tempered martensitic, lower bainitic and a combination of tempered martensitic and lower bainitic microstructures. Heat treatments were basically designed to compare the mechanical properties of resulting microstructures having similar hardness values.

The tempering route applied to the quenched specimens is shown in Figure 4.3 After the specimens were austenitized at 860°C for 30 minutes and quenched in water, the tempering temperature T_t is set to either 220°C (5 hours), 450°C (1,5 hours), 500°C (1,5 hours) or 550°C (1,5 hours). Finally, samples were quenched in oil.

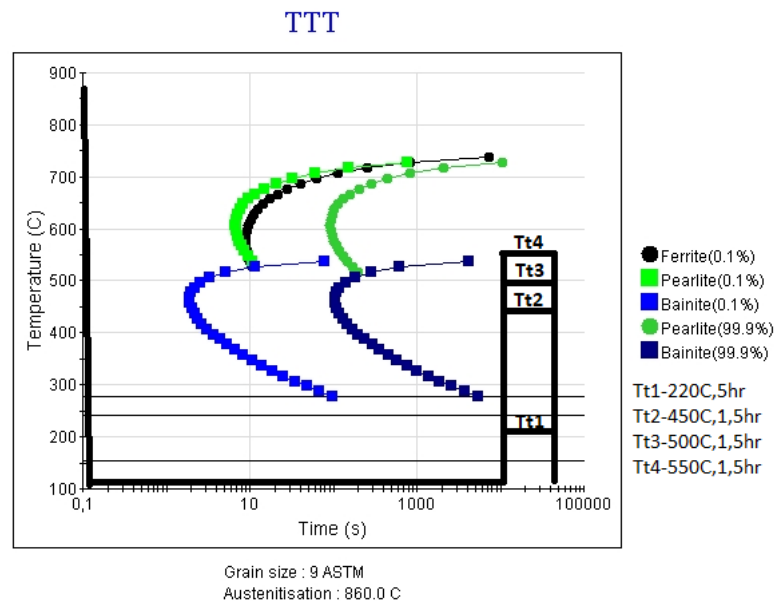


Figure 4.3. Routes for tempered martensitic microstructures of 55Cr3

Lower bainitic microstructures were achieved by holding the specimen at just above M_s . As shown in Figure 4.4, the samples were isothermally held at 270°C for 8 minutes, 80 minutes or 3 hours in order to monitor the lower bainitic transformation.

TTT

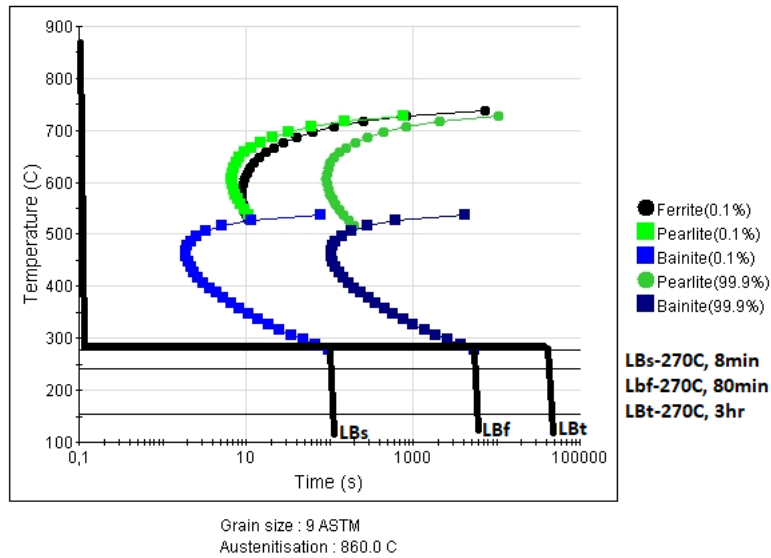


Figure 4.4. Routes for lower bainitic microstructures of 55Cr3

In addition, another sample was held at around M_{50} temperature, i.e. at 240°C, for 5 hours to achieve a combination of tempered martensite and lower bainite in the same specimen as shown in Figure 4.5. The heat treatment time was set by extrapolation of bainite finish curves on TTT. All the heat treatments applied to 55Cr3 samples and the designated short notations of each specimen are summarized in Table 4.2. The assumed microstructures are also included to the table.

TTT

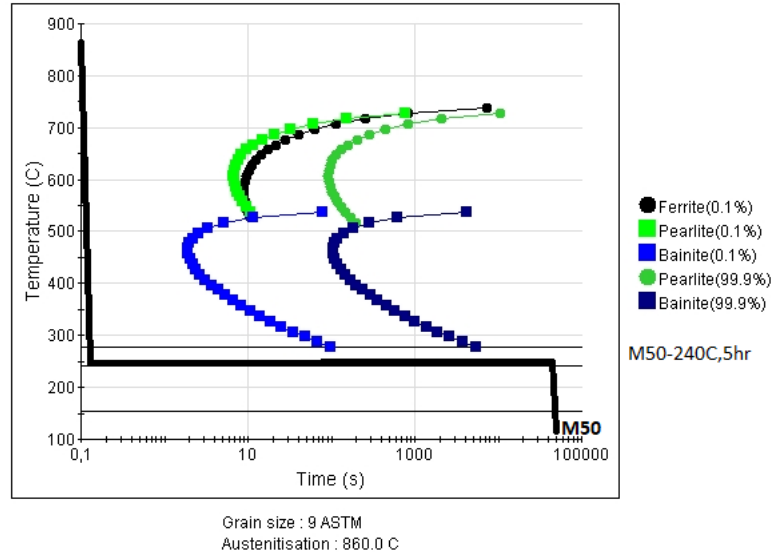


Figure 4.5. Route for under M₅₀ treatment for 55Cr3 steel

Table 4.2. Heat treatment routes for 55Cr3

Q&T Treatment	Notation	Quench Media	Microstructure
220°C, 5 hours	220°C, 5hr	Oil	TM
450°C, 1,5 hours	450°C, 1.5hr	Oil	TM
500°C, 1,5 hours	500°C, 1.5hr	Oil	TM
550°C, 1,5 hours	550°C, 1.5hr	Oil	TM
Isothermal Treatment			
270°C, 8 minutes	270°C, 8min	Water	LB
270°C, 80 minutes	270°C, 80min	Water	LB
270°C, 3 hours	270°C, 3hr	Water	LB
Under M_s Treatment			
240°C, 5 hours	240°C, 5hr	Water	TM + LB

4.3. Heat Treatment of 60SiMn5

After austenitization at 860°C for 30 minutes, 60SiMn5 samples were subjected to the treatments illustrated Figure 4.6 in order to obtain lower bainite. The heat treatment applied to 60SiMn5 samples and the designated short notation of the specimen is summarized in Table 4.3.

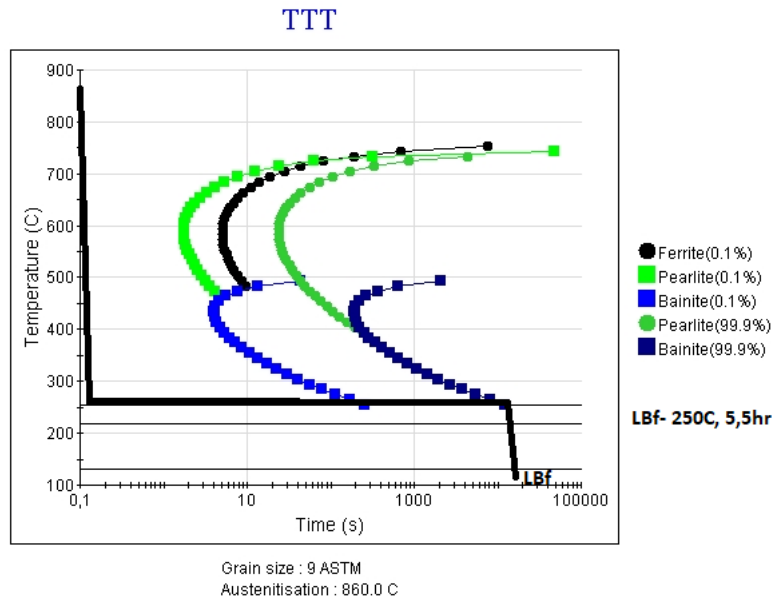


Figure 4.6. Route for lower bainite transformation of 60SiMn5

Table 4.3. Heat treatment route for 60SiMn5

<i>Isothermal Treatment</i>	<i>Notation</i>	<i>Quench Media</i>	<i>Microstructure</i>
250°C, 5.5 hours	250°C, 5.5hr	Water	LB

4.4. Microstructural Examinations

The microstructural examination of tempered martensite, lower bainite, the combination of tempered martensite and lower bainite of 55Cr3 steel were done. In addition, the tempered martensite and lower bainite of 60SiMn5 steel were also

examined in this section. Examinations were done by optical microscope for martensite; while both optical microscope and SEM were used for lower bainite.

4.4.1. Microstructural Examinations for 55Cr3

4.4.1.1. Martensitic Transformation in 55Cr3

The Figures given below illustrates the images of as-quenched and tempered martensite samples under optical microscope and SEM. In as-quenched condition, there is a banded microstructure as shown in Figure 4.7. This banded microstructure has already been observed in as-received samples, as well. In tempered samples as shown in Figure 4.8, Figure 4.9, Figure 4.10, and Figure 4.11 this banded microstructure become less visible but still exists. The banded microstructure is most probably due to the segregation of Cr.

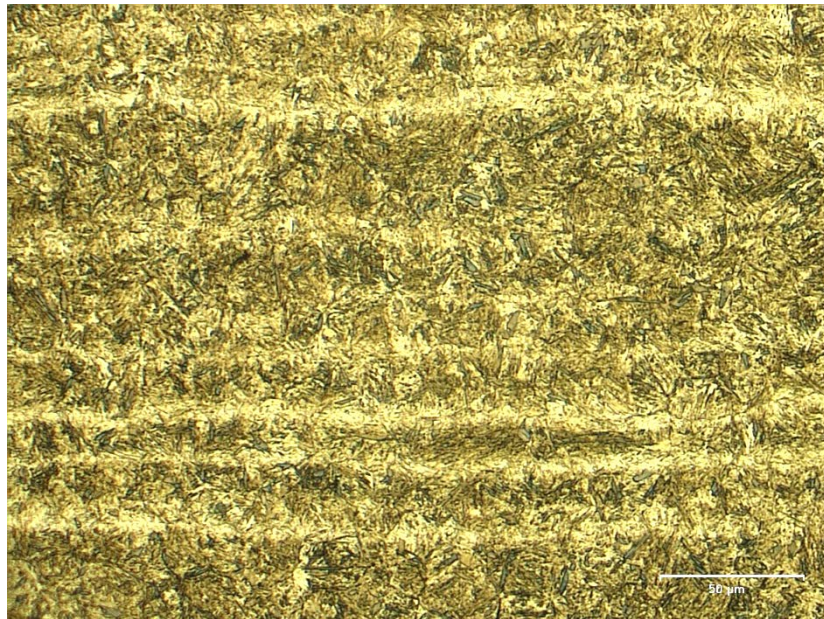


Figure 4.7. As-quenched martensite

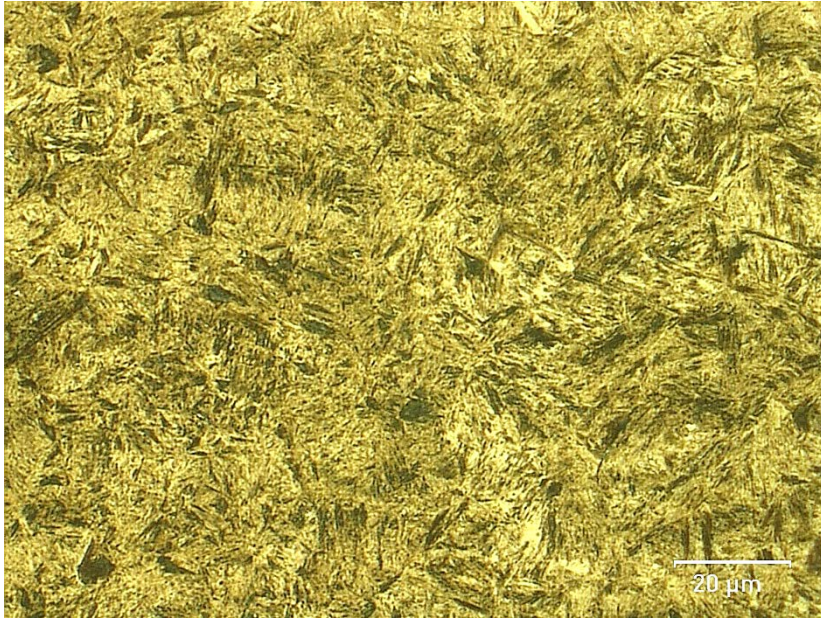


Figure 4.8. The optical micrograph of tempered martensite. (220°C, 5hrs)



Figure 4.9. The optical micrograph of tempered martensite. (450°C, 1,5hr)



Figure 4.10. The optical micrograph of tempered martensite. (500°C, 1,5hr)



Figure 4.11. The optical micrograph of tempered martensite. (550°C, 1,5hrs)

4.4.1.2. Lower Bainitic Transformation

55Cr3 samples were firstly treated to obtain the beginning of the lower bainite formation. Although TTT diagram dictates that bainite starts to form approximately in 8 minutes at 270°C, the microstructures taken under optical microscope (Figure 4.12) showed that the transformation rate is so high that the bainite transformation is nearly complete even in 8 minutes. This indicates that the readings from TTT diagrams that have been generated by JMatPro® software may have some slight deviations from the real time situations. The white matrix under the bainitic ferrite needles is the austenite phase which is transformed to martensite upon cooling to room temperature.

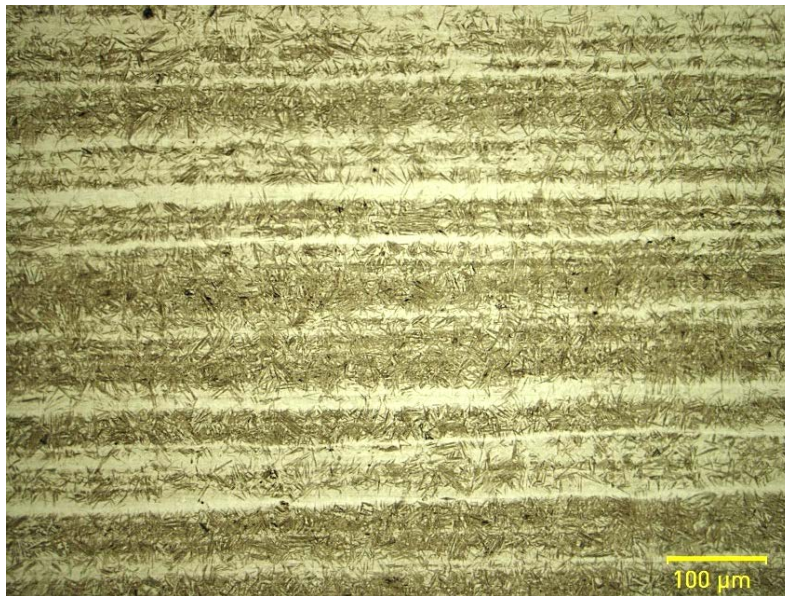


Figure 4.12. Isothermally treated (270°C, 8min). Lower bainite needles (dark) together with martensite phase (white matrix).

Bainitic ferrite plates (dark) and martensitic matrix (white) can be seen easily in Figure 4.13. The bands due to Cr also exists in bainitic microstructure.

According to the TTT diagram for 55Cr3, bainite formation should be completed in 80 minutes at 270°C. For this reason, another specimen was isothermally held at 270°C for 80 minutes. Figure 4.14 and shows that the microstructure is fully bainitic.

Another specimen was isothermally held at 270°C for 3 hours in order to obtain tempered lower bainite (Figure 4.15). Figure 4.16 and Figure 4.17 illustrates with a higher magnification that the formerly transformed lower bainite sheaves seem darker compared to the ones formed at a later stage.

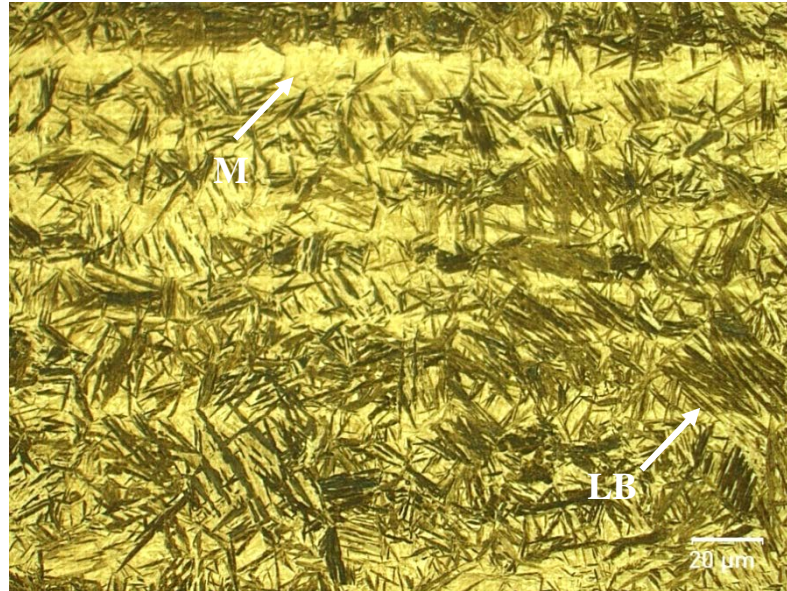


Figure 4.13. Optical micrograph of isothermally treated specimen at 270°C for 8 min

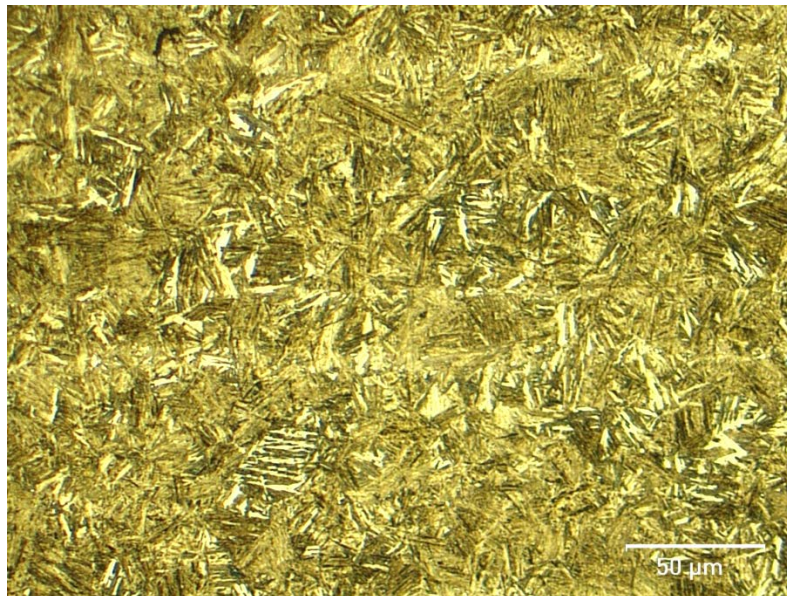


Figure 4.14. Optical micrograph of isothermally treated specimen at 270°C for 80 min. Bainite transformation is completed.



Figure 4.15. Optical micrograph of isothermally held sample at 270°C for 80 min.



Figure 4.16. Optical micrograph of isothermally held sample at 270°C for 3 hrs.

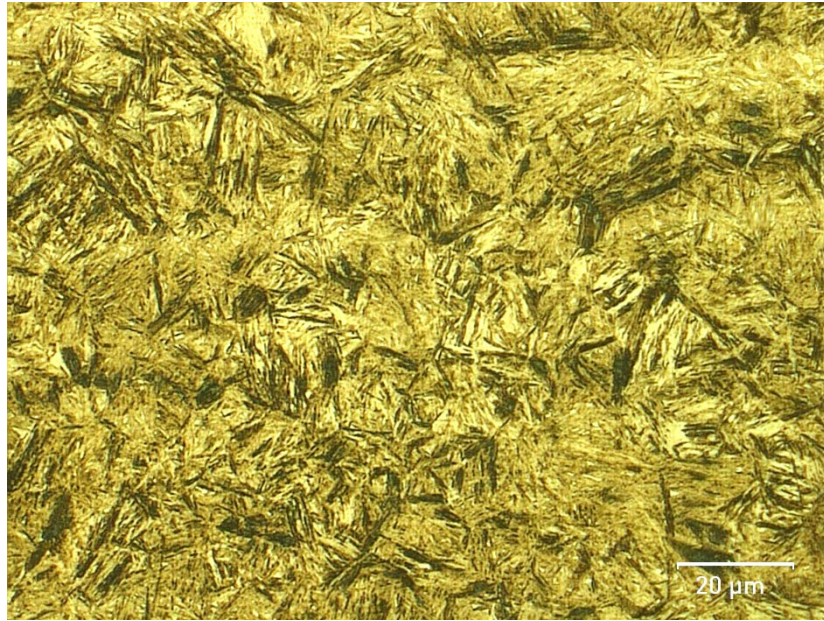


Figure 4.17. Optical micrograph of isothermally held sample at 270°C for 3 hrs.

4.4.1.3. Isothermal Transformations Below M_s Temperature

In this heat treatment the coexistence of lower bainite and tempered martensite is aimed. After austenitization, samples were directly quenched in a salt bath at 240°C and held at that temperature for 5 hours. The purpose was to obtain 50% martensitic-50% bainitic microstructure since the specimen was quenched to M_{50} temperature. The specimen kept at the same temperature for 5 hours, which is the time required to complete bainitic transformation at 240°C according to the calculated TTT diagram. During this period, the formerly transformed martensite is expected to be tempered. Hence, although it was difficult to differentiate tempered martensite and lower bainite at every region, at several locations a mixture of martensite-bainite could be observed (Figure 4.18 and Figure 4.19).

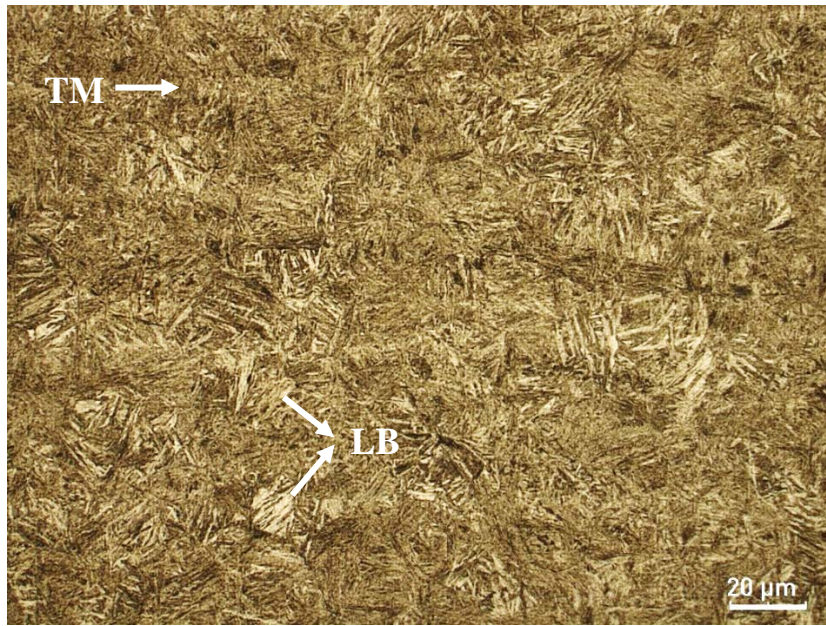


Figure 4.18. Optical micrograph of isothermally treated sample at M_{50} 270°C for 3 hrs



Figure 4.19. Optical micrograph of isothermally treated sample at M_{50} 270°C for 3 hrs

4.4.2. Phase Transformations in 60SiMn5

Samples made of 60SiMn5 steel were heat treated to achieve the lower bainitic microstructure as shown in Figure 4.20.

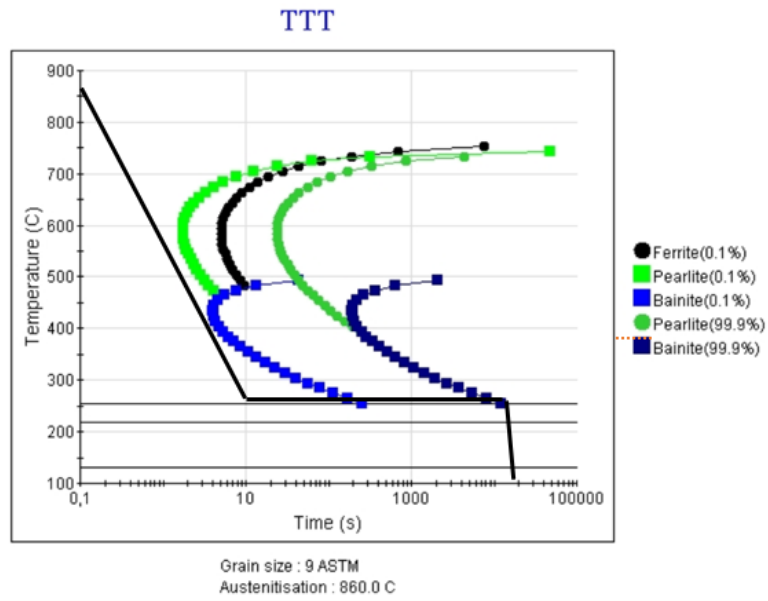


Figure 4.20. The route for lower bainitic microstructure of 60SiMn5

4.4.2.1. Lower Bainitic Transformation

The lower bainitic microstructure of 60SiMn5 isothermally held at 250°C for 5,5 hours can be seen in Figure 4.21 and Figure 4.22.

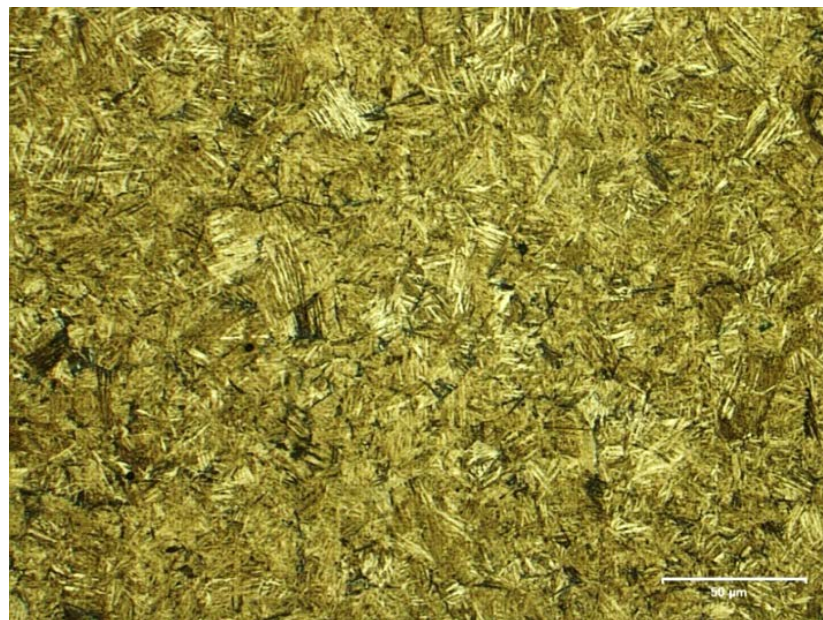


Figure 4.21. Optical micrograph of isothermally held sample at 250°C for 5,5hrs.

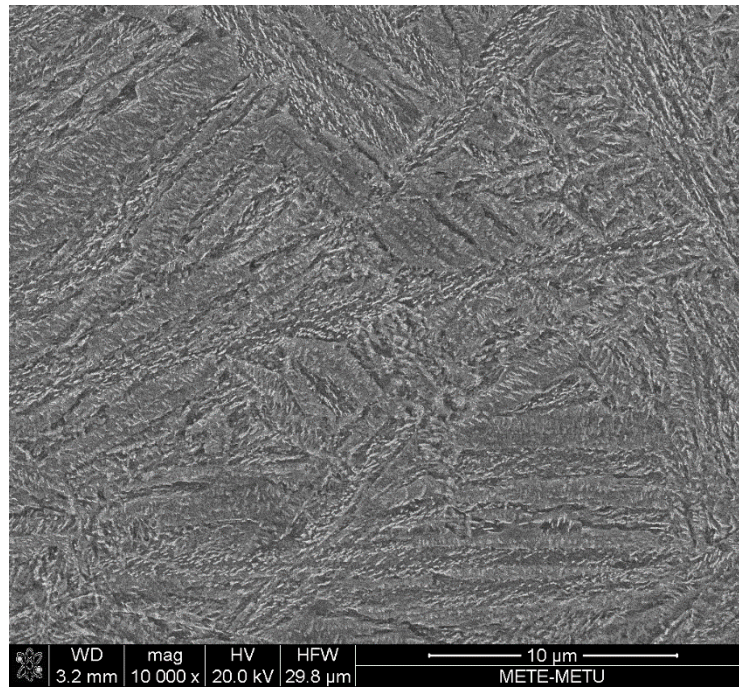


Figure 4.22. Optical micrograph of isothermally held sample at 250°C for 5,5 hrs.

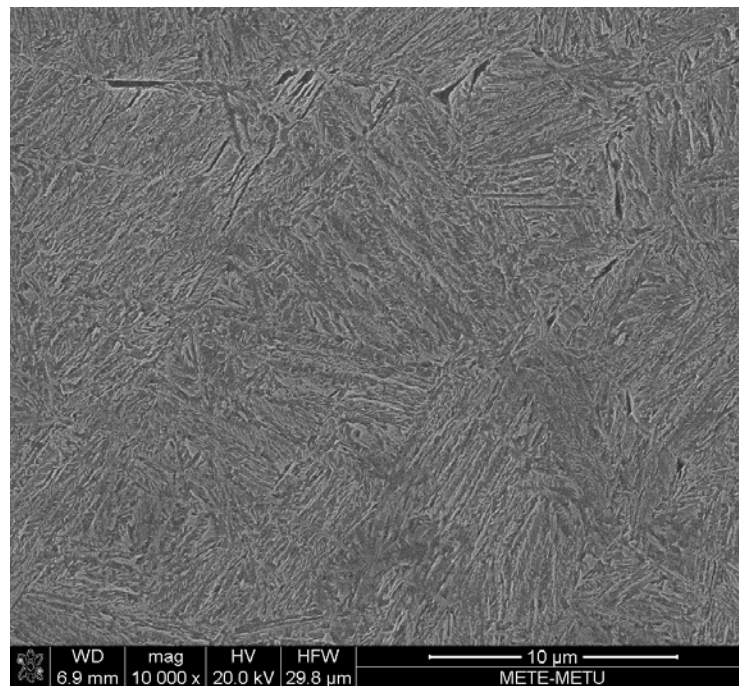
4.4.3. Comparison of Lower Bainitic Microstructures of 55Cr3 and 60SiMn5 under SEM

In order to make a detailed comparison of lower bainitic microstructures of 55Cr3 and 60SiMn5 steels, the specimens were observed under SEM.

Figure 4.23 illustrates the differences between lower bainite of 55Cr3 and 60SiMn5. The carbide precipitates in bainitic structure of 55Cr3 are apparently visible especially at high magnifications in Figure 4.24 (a) and Figure 4.24 (c). However, there is no carbide precipitate in the lower bainite of 60SiMn5 as shown in Figure 4.24 (b) and Figure 4.24 (d). This is the reason why the lower bainite of 60SiMn5 is named as “carbide-free lower bainite”. Besides carbide precipitation, there are few austenite islands (which probably transformed to martensite upon cooling) are seen in Figure 4.24 (b). These islands are generally called M/A, as they may retain as austenite or transform to martensite upon cooling to room temperature

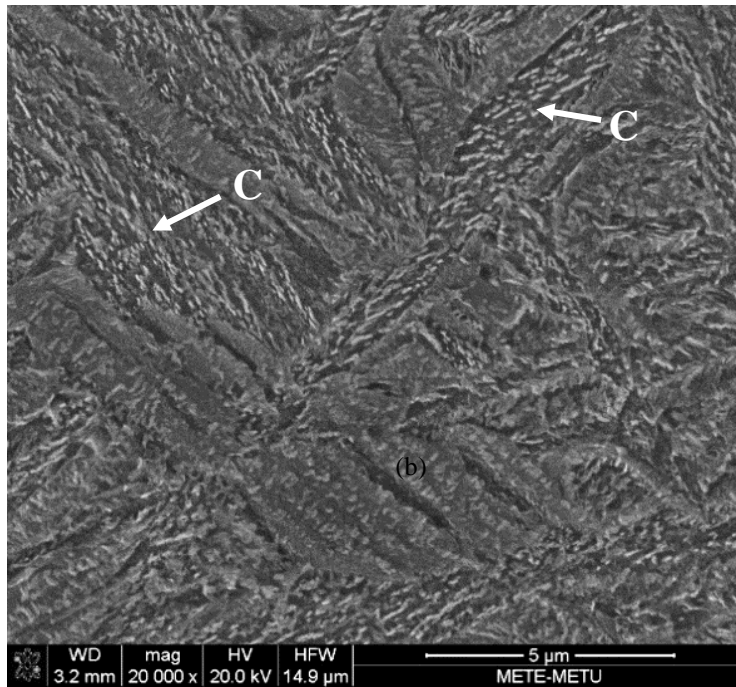


(a)

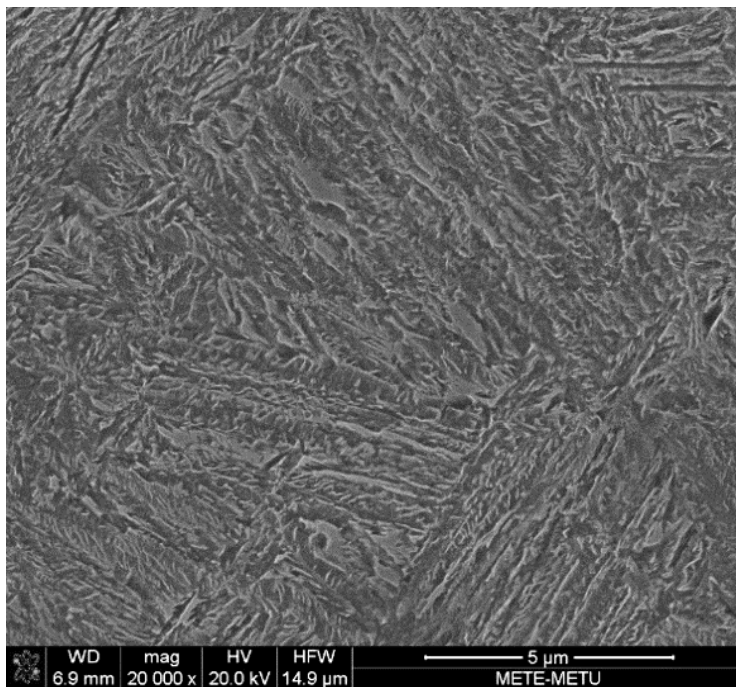


(b)

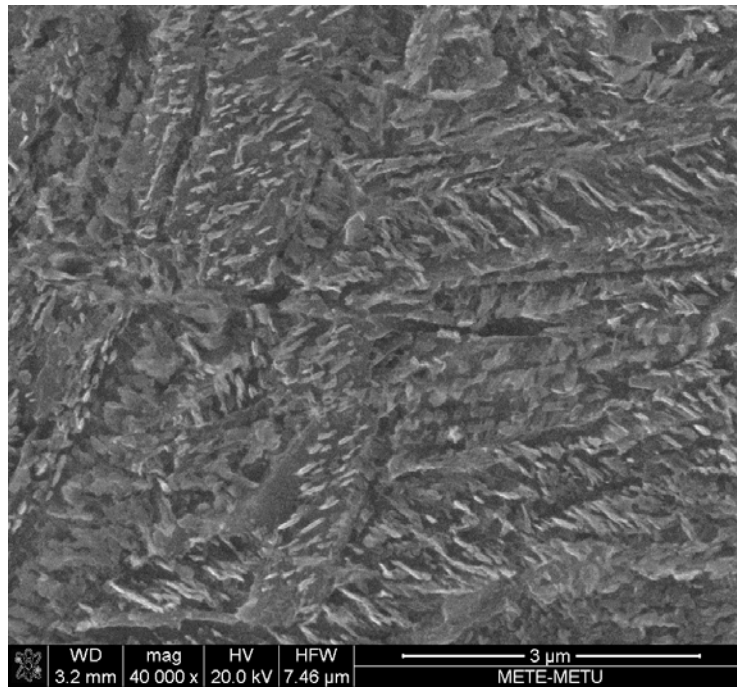
Figure 4.23. SEM micrographs of (a) 55Cr3 lower bainite, 270°C 80min, (b) 60SiMn5 lower bainite, 250°C 5,5hr



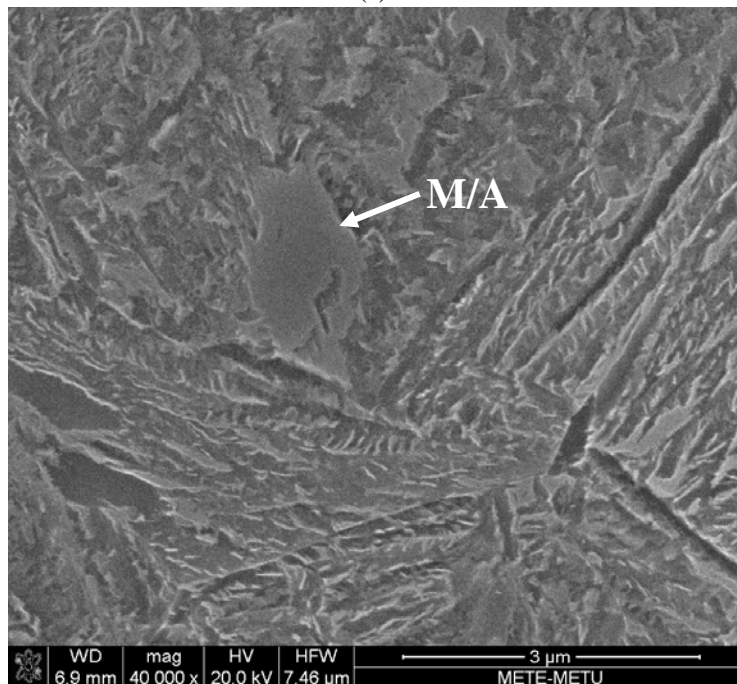
(a)



(b)



(c)



(d)

Figure 4.24. SEM micrographs of (a) & (c) 55Cr3 lower bainite with carbides (270°C 80min), (b) & (d) 60SiMn5 lower bainite (250°C 5,5hr). Carbides are seen in 55Cr3, whereas no carbides are seen in 60SiMn5 specimen

4.5. Mechanical Test Results

4.5.1. Hardness Tests

The results for the hardness tests applied to 55Cr3 heat treated steels are shown in Table 4.4 and plotted in Figure 4.25. As seen, as-quenched sample yielded 770HV hardness and the hardness values decreased as the tempering temperature increased. The highest hardness value among the tempered samples is 653HV for “220°C,5hr” sample. The as-quenched martensite is not considered since non-tempered martensite is not common in industry due to its high brittleness and low toughness.

For bainitic transformations, the hardness values decrease as the isothermal transformation times increase. In other words, the hardness decreases as the amount of lower bainite increases. The “270°C, 8min” sample has the highest hardness value with 635HV since it has less lower bainite and contains fresh martensite. The “270°C, 80min” sample contains 100% lower bainite and has 583HV.

The “240°C, 5hr” sample contains both tempered martensite and lower bainite and yields 614HV hardness. Upon quenching to 240°C will form some amount of martensite, as Ms is crossed. When the isothermal transformation continues at 240°C, the remaining austenite will transform to bainite and the initially formed martensite will be tempered in the same period. The samples having similar hardness values are the main target to make comparison between all mechanical properties.

Table 4.4. Hardness test results for 55Cr3 and 60SiMn5 samples

Q&T Treatment	Microstructure	Hardness (HV30)
Q	M	770 ±4
220°C, 5hr (55Cr3)	TM	653 ±5
450°C, 1.5hr (55Cr3)	TM	480 ±3
500°C, 1.5hr (55Cr3)	TM	435 ±6
550°C, 1.5hr (55Cr3)	TM	396 ±4
Isothermal Treatment		
250°C, 5.5hr (60SiMn5)	LB	601 ±7

270°C, 8min (55Cr3)	LB	635 ±7
270°C, 80min (55Cr3)	LB	583 ±8
270°C, 3hr (55Cr3)	LB	570 ±7
<hr/>		
Below M_s Treatment		
240°C, 5hr (55Cr3)	TM & LB	614 ±6
<hr/>		

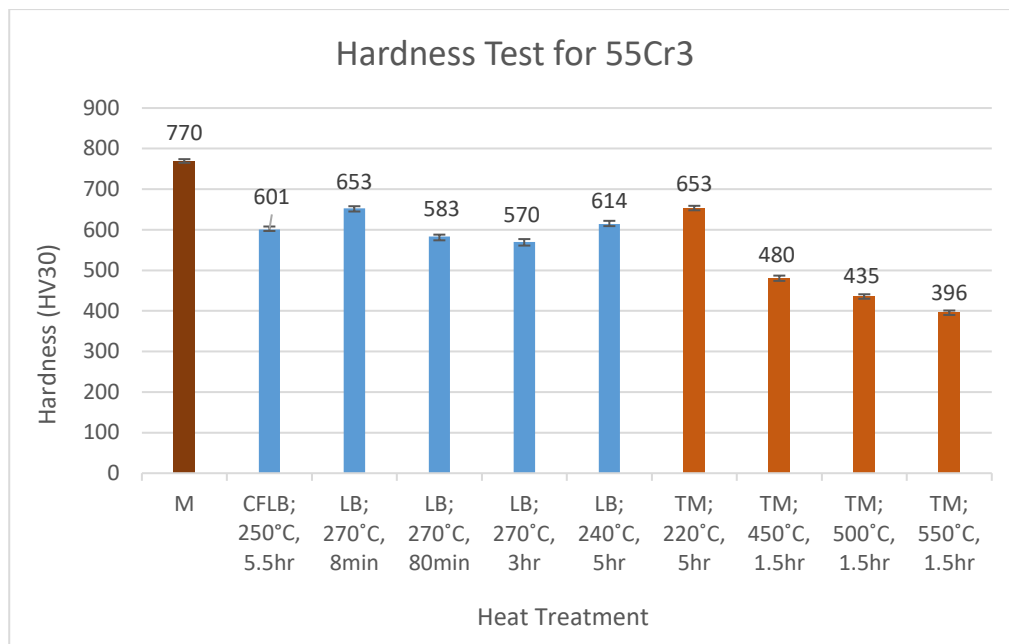


Figure 4.25. Hardness values of 55Cr3 samples after application of various heat treatment routes.

From the results both in Table 4.4 and Figure 4.25, it is seen that the hardness values of 100% lower bainitic samples are greater than that of tempered martensitic samples. Moreover, the 100% lower bainitic sample of 60SiMn5 has the hardness of 601HV, which is slightly higher than that of 55Cr3.

4.5.2. Tensile Tests

The tensile test results for 55Cr3 and 60SiMn5 (250°C, 5.5hr) samples are summarized in Table 4.5. The result for 60SiMn5 carbide-free lower bainite was shown as “250°C, 5,5hr (CFLB)” in the table. Results show that fully lower bainitic samples which were obtained by isothermal treatment at 270°C for either 80 minutes or 3 hours yielded

very close yield strength and ultimate tensile strength values. They have the highest yield and ultimate tensile strength values among all other specimens. Surprisingly, although fresh martensite is present in the microstructure together with bainite, the sample that was isothermally treated at 270°C for only 8 minutes gave the yield and ultimate tensile strength values that is almost equal with or higher than that of tempered martensite samples.

Except that the specimen tempered at 220°C, other tempered martensitic samples show a decreasing trend in both yield and tensile strengths, as the tempering temperature increases. However, the tempered sample at 220°C, ruptured at a very low UTS value without any elongation during the test.

Table 4.5. Tensile test results for 55Cr3 & 60SiMn5 samples

Q&T Treatment	Hardness (HV30)	Yield Strength (MPa)	Ultimate Tensile Strength (MPa)	Elongation (%)
220°C, 5 hr (55Cr3)	653	0	302	0,2
450°C, 1,5 hr (55Cr3)	480	1222	1269	0,9
500°C, 1,5 hr (55Cr3)	435	992	1018	0,9
550°C, 1,5 hr (55Cr3)	396	986	1011	1,4
Isothermal Treatment				
250°C, 5,5hr (60SiMn5)	601	1781	2107	5,68
270°C, 8 min (55Cr3)	635	1187	1263	0,89
270°C, 80 min (55Cr3)	583	1645	1984	12,3
270°C, 3 hr (55Cr3)	570	1638	1961	10,5
Below M_s Treatment				
240°C, 5 hr (55Cr3)	614	1429	1600	0,93

Results show that 100% lower bainite specimens (80 min and 3 hrs) have significantly high yield strength and ultimate tensile strength values when compared to the other specimens. They have also very close %elongation values. It was unexpected that even there is fresh martensite in the microstructure, the 240°C sample has showed good

yield and ultimate tensile strength values. However, its strain value is low among other tempered martensite samples.

The fracture surfaces of tempered martensitic samples after tensile testing are illustrated in Figure 4.26 for 220°C, 5hr and in Figure 4.27 for 450°C, 1.5hr. When examined, it is seen that the fracture surface is transformed from brittle to ductile morphology as tempering temperature is increased from 220°C to 450°C.

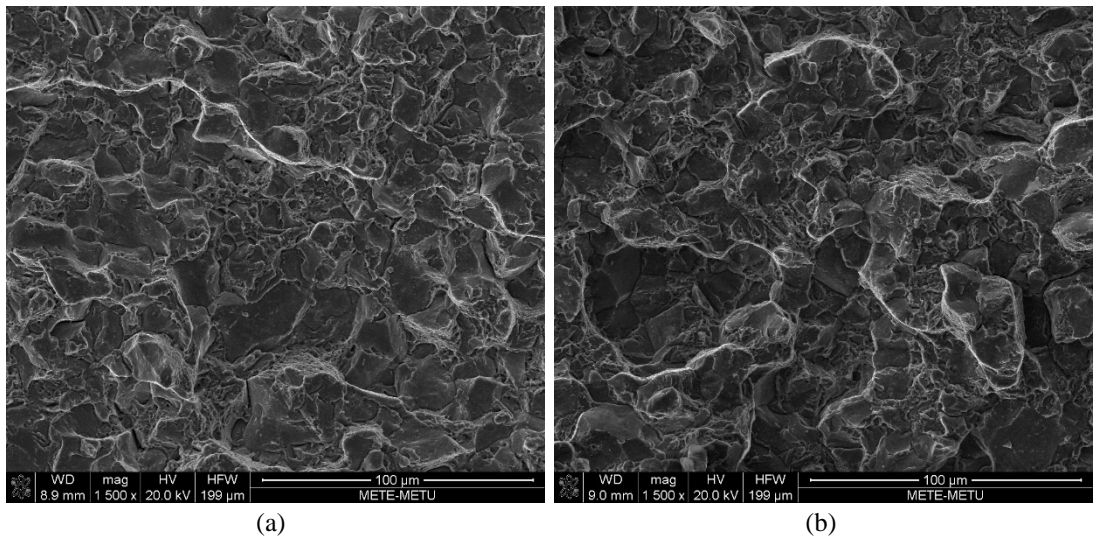


Figure 4.26. Fracture surfaces of the tensile test specimens quenched and tempered at 220°C, 5hr.

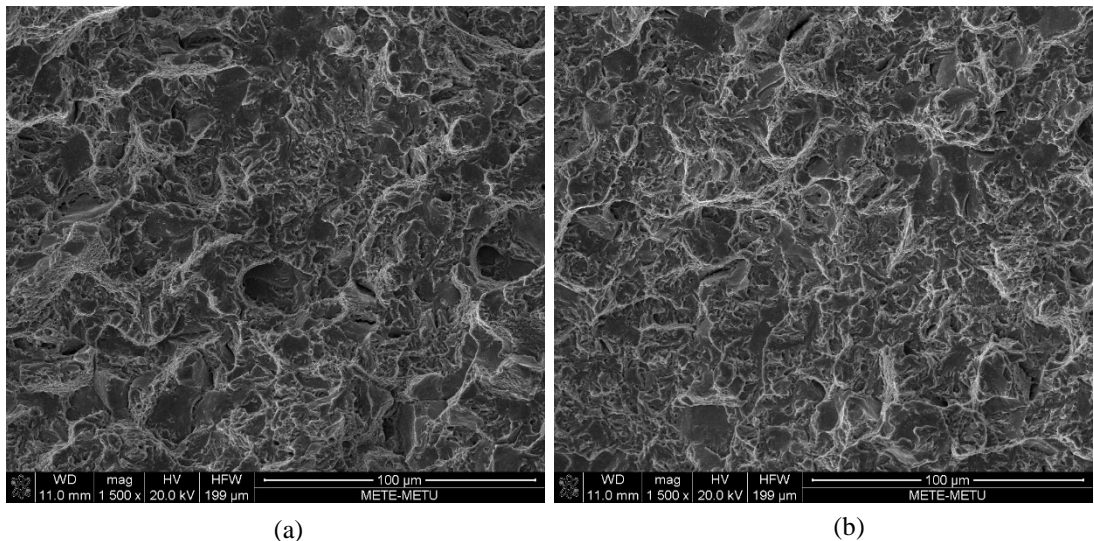


Figure 4.27. Fracture surfaces of the tensile test specimens quenched and tempered at 450°C, 1.5hr.

The fracture surfaces of specimens treated at 270°C (80min) and at 240°C (5hrs) are compared in Figure 4.28 and Figure 4.29. As shown previously, 270C (80 mins) specimen is 100% bainitic, but specimen 240C (5hrs) consists of bainite-martensite phase mixture. As seen, the bainitic specimen has a ductile fracture morphology (Figure 4.28) but bainitic-martensitic specimen has mostly intergranular type of fracture surface (Figure 4.29). In quenched and tempered steels, intergranular fracture is typical if the specimen is not tempered or if tempering is not sufficient.

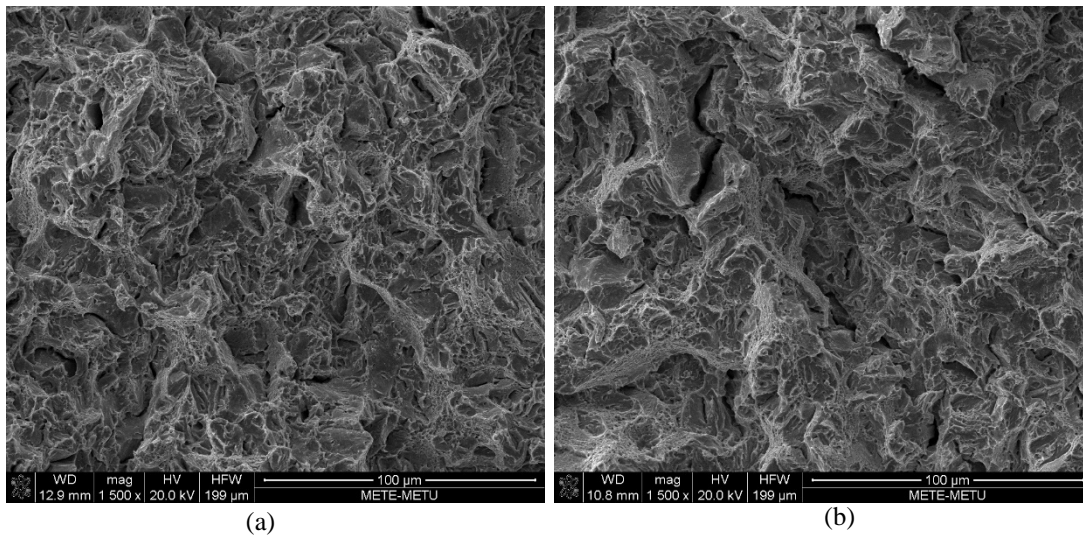


Figure 4.28. Fracture surfaces of the tensile test specimens of lower bainite transformed 270°C, 80min.

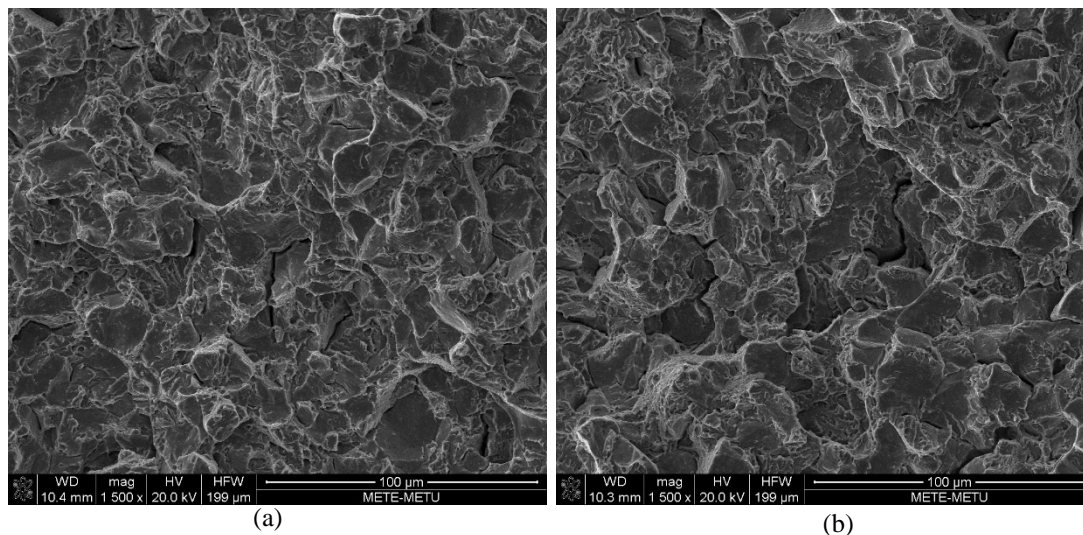


Figure 4.29. Fracture surfaces of the tensile test specimens of under M_s treatment at 240°C, 5hr.

The fracture surfaces of lower bainitic sample of 60SiMn5 after tensile test are shown in Figure 4.30. The fracture surfaces mostly consist of dimples but cleavages are also seen.

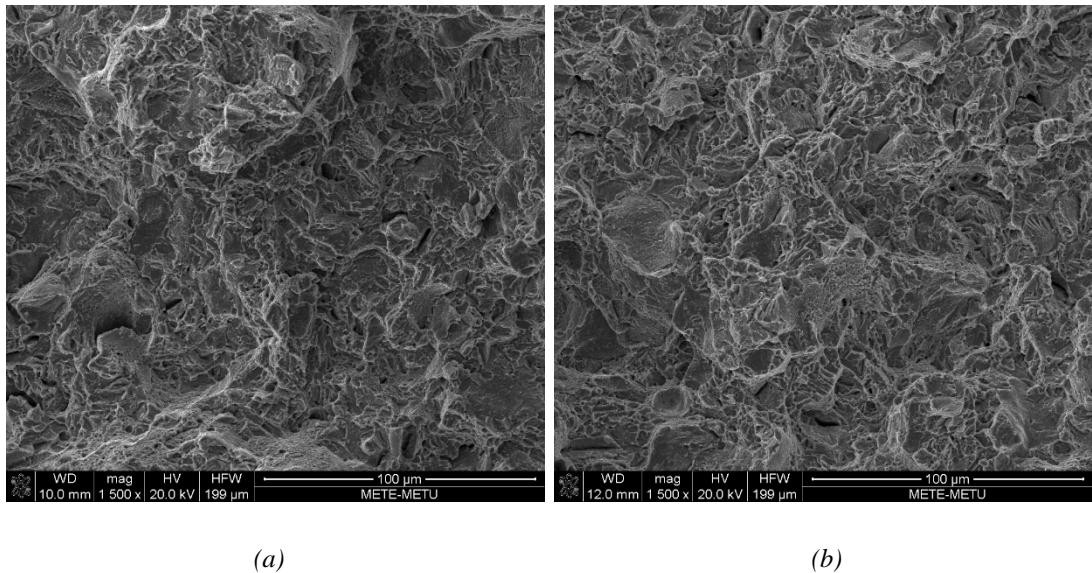


Figure 4.30. Fracture surfaces of the tensile test specimens of lower bainite transformed at 250°C, 5,5hr.

4.5.3. Charpy Impact Test Results

The notched bar impact test results for 55Cr3 and 60SiMn5 samples are tabulated in Table 4.6. Results show that except for 220°C tempering sample, the tempered martensite samples of 55Cr3 have the highest impact energies. The 450°C, 500°C, 550°C tempering samples have the impact energies of 20.7J, 21.7J, and 21J, respectively. Whereas, the 220°C tempering sample has only 3,3J. The 8 minute-isothermally treated sample has the lowest impact energy most probably due to the fresh martensite in its microstructure. The 80 minute and 3 hour-isothermally treated samples at 270C have an impact energy of 12,7 and 11,7J, respectively. The 240°C isothermally treated sample has 8,3J impact energy. The results are compared in Figure 4.31 Moreover, the Charpy impact test result for lower bainite of 60SiMn5 (250°C, 5.5hr) was measured as 9 Joule and the fracture surfaces of test specimens are shown in Figure 4.37..

Table 4.6. Charpy impact test results for 55Cr3 and 60SiMn5 samples

Q&T Treatment	Hardness (HV30)	Yield Strength (MPa)	Ultimate Tensile Strength (MPa)	Elongation (%)	Impact Energy (J)
220°C, 5hr (55Cr3)	653±5	0	302	0,2	3,3±1,7
450°C, 1,5hr (55Cr3)	480±3	1222	1269	0,9	20,7±2,4
500°C, 1,5hr (55Cr3)	435±6	992	1018	0,9	21,7±3,6
550°C, 1,5hr (55Cr3)	396±4	986	1011	1,4	21±2
Isothermal Treatment					
250°C, 5.5hr(60SiMn5)	600±7	1781	2107	5,68	9±1
270°C, 8min (55Cr3)	635±7	1187	1263	0,89	2,3±0,7
270°C, 80min (55Cr3)	583±8	1645	1984	12,3	12,7±0,6
270°C, 3hr (55Cr3)	570±7	1638	1961	10,5	11,7±1,4
Below M _s Treatment					
240°C, 5hr (55Cr3)	614±6	1429	1600	0,93	8,3±1,7

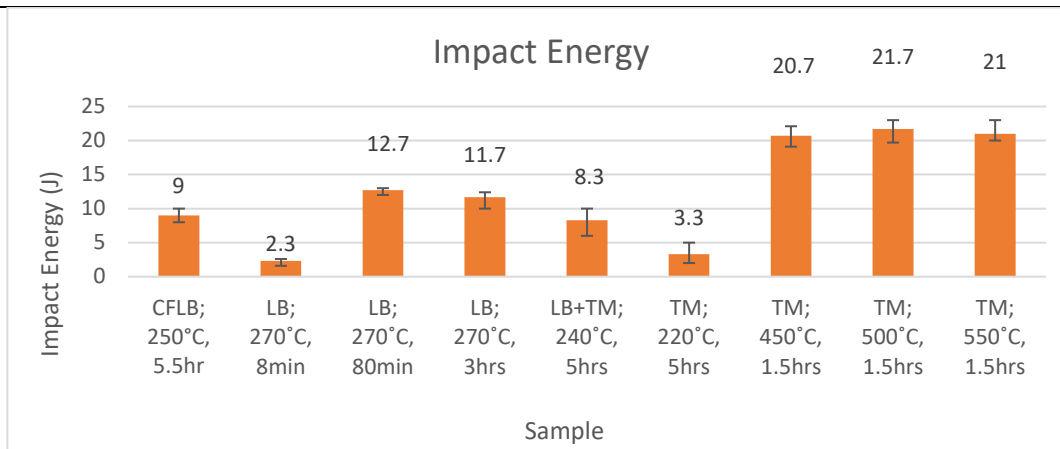


Figure 4.31. Graph for impact energy values of 55Cr3 and 60SiMn5 samples

The fracture surfaces of notched bar Charpy impact test samples were analyzed under SEM. Figure 4.32 and Figure 4.33 shows, there are mostly dimples on tempered martensite samples. Figure 4.34 and Figure 4.37 illustrate that the fracture types are

mostly like cleavage-type, yet still containing dimples for lower bainite of both 55Cr3 and 60SiMn5 steels. The dimples are more visible in Figure 4.35 and Figure 4.38 which were taken at higher magnification. The sample treated under M_s temperature (240°C, 5hr) has also mostly cleavage-type fracture as seen in Figure 4.36.

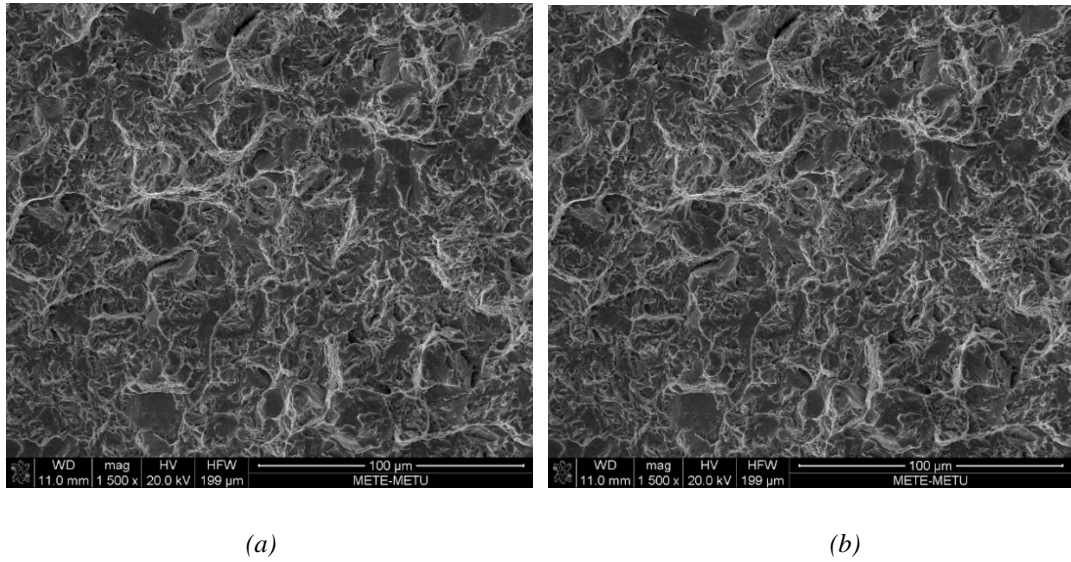


Figure 4.32. Fracture surfaces of Charpy impact test specimens of tempered martensite at 450°C, 1,5hr

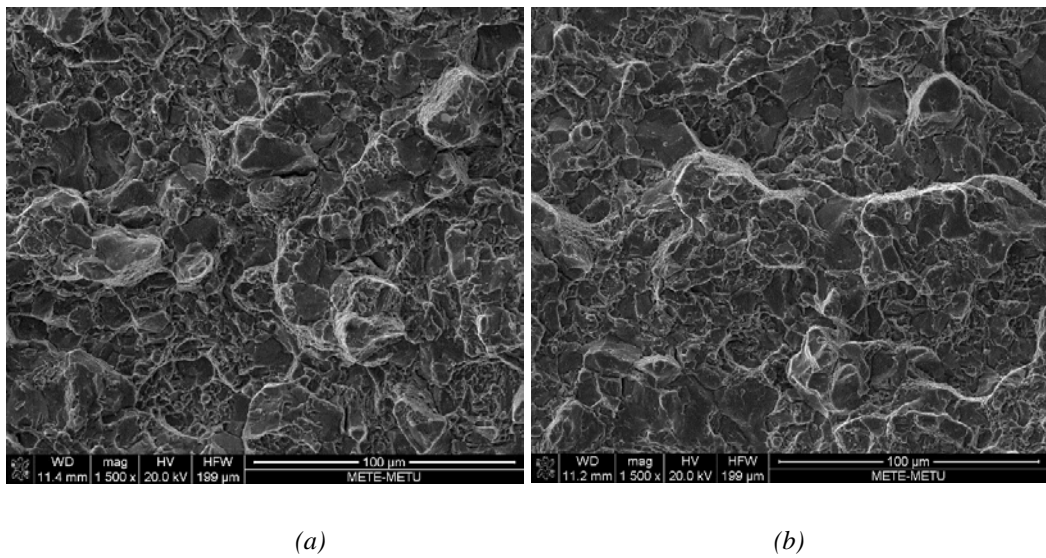
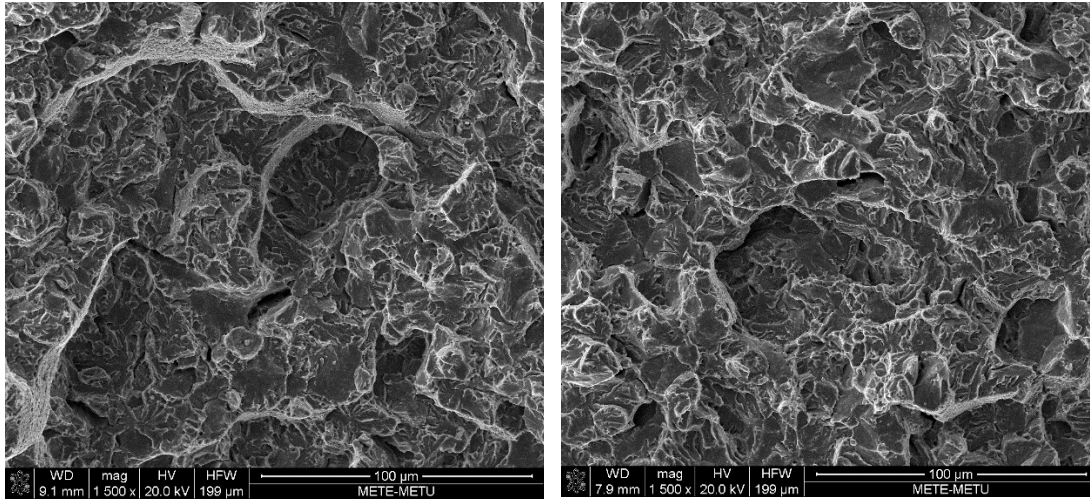


Figure 4.33. Fracture surfaces of Charpy impact test specimens of tempered martensite at 220°C, 5hr.



(a)

(b)

Figure 4.34. Fracture surfaces of Charpy impact test specimens of lower bainite transformed at 270°C, 80min.

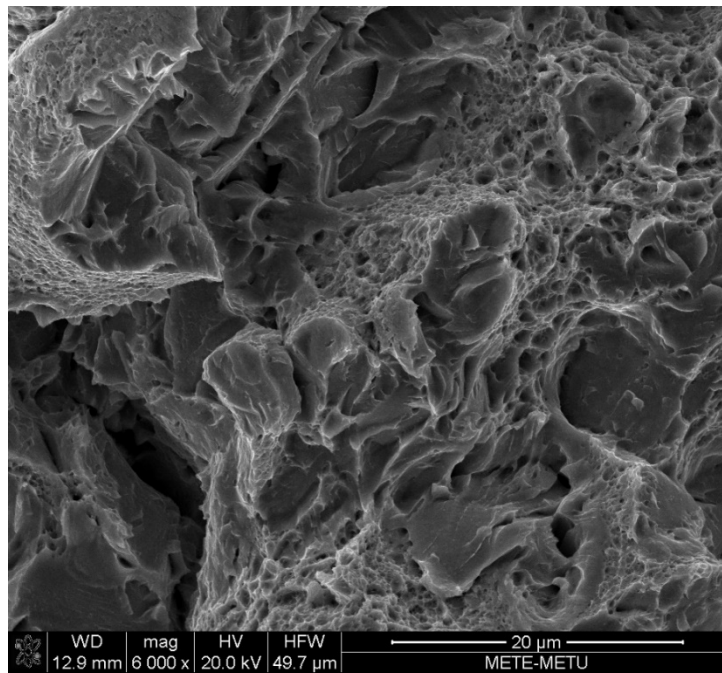
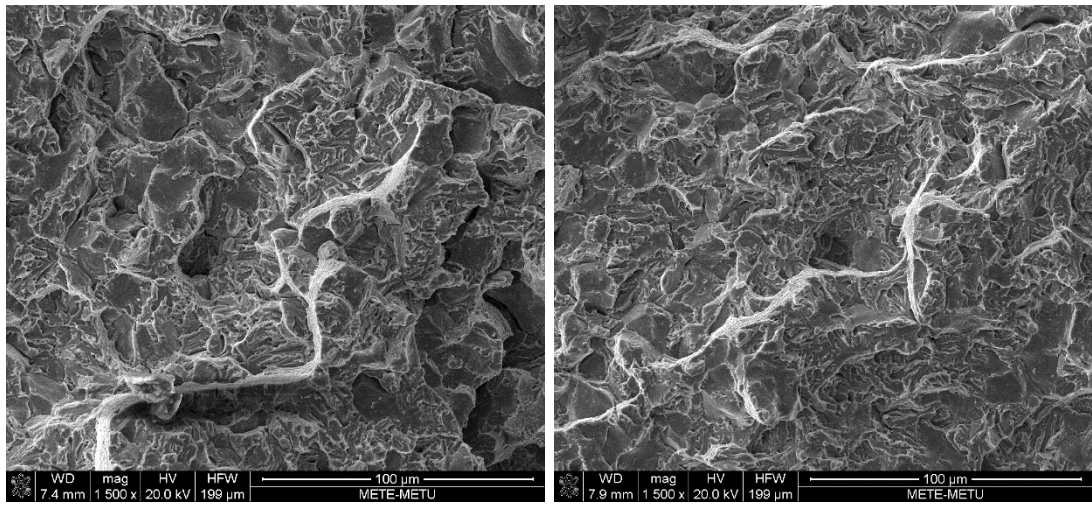


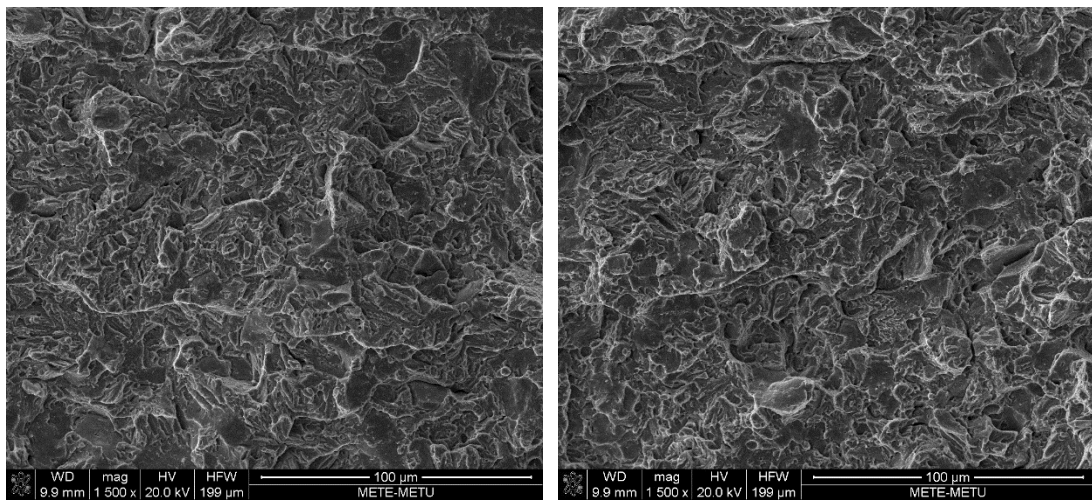
Figure 4.35. Fracture surfaces of Charpy impact test specimens of lower bainite transformed at 270°C, 80min (higher magnification).



(a)

(b)

Figure 4.36. Fracture surfaces of Charpy impact test specimens of under M_s treatment at 240°C, 5hr



(a)

(b)

Figure 4.37. Fracture surfaces of Charpy impact test specimens of carbide-free lower bainite of 60SiMn5 Mn5 transformed at 250°C, 5.5hr.

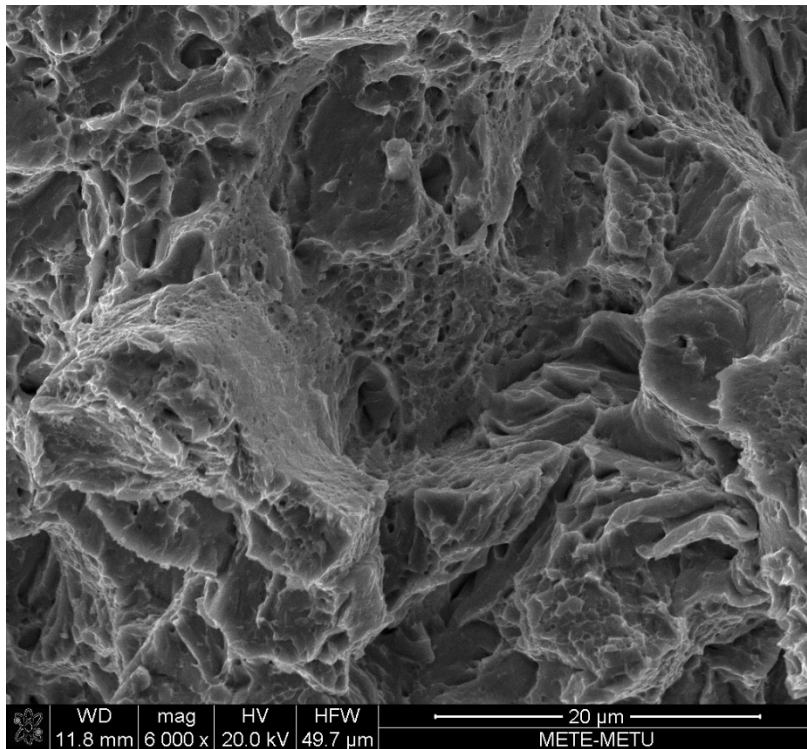


Figure 4.38. Fracture surfaces of Charpy impact test specimens of carbide-free lower bainite of 60SiMn5 transformed at 250°C, 5.5hr. (higher magnification).

From the data in Table 4.6, it can be that there is a slight difference between the impact energy values of lower bainitic microstructures of both steels. While the lower bainite of 55Cr3 has 12,7J impact energy, lower bainite of 60SiMn5 has 9J impact energy. These values are very close to each other and both steels can be assumed to have almost the same impact energy values.

CHAPTER 5

DISCUSSION

In this study, 55Cr3 and 60SiMn5 steels, which are known as spring steels, were used to obtain tempered martensitic and lower bainitic microstructures to compare their mechanical properties. The comparison was firstly based on the martensitic and bainitic microstructures of 55Cr3 steel which had similar hardness values. Then lower bainitic structures of 55Cr3 and 60SiMn5 were compared.

All of the experiments were done according to the TTT diagrams generated by JMatPro[®] software for each steel. After preliminary experiments, the heat treatment parameters were set and it was seen that the resulting microstructures were consistent with the calculated TTT diagrams. The routes for the tempered martensite, the lower bainite and under M_s treatments of 55Cr3 were shown in Figure 4.3, Figure 4.4, Figure 4.5 respectively and for lower bainite treatment for 60SiMn5 is shown in Figure 4.6.

5.1. Microstructural Characterization of 55Cr3 and 60SiMn5

As mentioned in the previous chapter, 3 different isothermal treatment routes were applied to 55Cr3. Although it was predicted from the graph that bainite formation would start at 270°C after 8 minutes, the microstructures revealed that bainite starts to form even earlier than this period. Figure 4.13 shows that besides the martensitic matrix in white regions, there is a high amount of bainite sheaves which can be seen as dark. The predicted time for the completion of lower bainite was 80 minutes and the microstructure shown in Figure 4.14 seems almost fully bainitic. For the sample that was kept at 270°C for 3 hours, the lower bainitic microstructure was expected to be auto-tempered. In Figure 4.17, there are dark needles which can either be assumed as tempered bainite sheaves or martensite needles that are formed upon cooling to room temperature. Moreover, as it is seen from Figure 4.18 and Figure 4.19, cooling below M_s but above M_f resulted in martensitic-bainitic microstructures.

The microstructure in Figure 4.37. revealed that also the heat treatment for lower bainite of 60SiMn5 which was predicted as 250°C for 5,5hours was consistent.

In both martensitic and bainitic microstructures of 55Cr3 steel, the banded microstructures which are aligned parallel to the rolling direction of steel are remarkably seen in Figure 4.7 and Figure 4.13. It is known that the alloying elements like Cr, Mn and Mo have a tendency for segregation which cause banded structure after hot rolling. Therefore, as well as pearlite region in TTT diagram, the bainitic transformation also shifts to later stages. Thus, within the Cr-rich regions retardation of bainite will cause formation of martensite upon cooling to room temperature. The regions depleted in Cr transforms into martensite slower than the regions rich in Cr. Therefore, a banded microstructure of Cr-rich and Cr-depleted regions is seen. [36].

The main difference between tempered martensite and lower bainite comes from the location of cementite precipitates. The lower bainitic microstructure comprises of bainitic ferrite and embedded cementite platelets. Tu et. al. stated that the cementite precipitates at an angle of 55-60° to the long axes of ferrite and on the {0 1 1} habit plane of bainitic ferrite sheaves. On the other hand, in tempered martensite, cementite precipitates on twin planes which lie on {1 1 2} plane [37]. The carbide precipitates are well defined in Figure 4.24 (a) and (c) for lower bainite of 55Cr3 and seen that they are oriented at an angle within ferrite sheaves. However, although the cementite is hardly differentiated in martensitic sample of 55Cr3 as seen in Figure 5.1. the orientation difference can easily be seen when the it is examined under TEM.

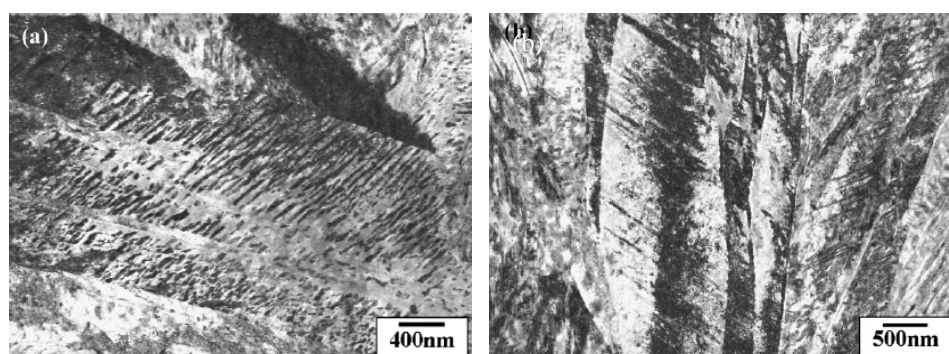


Figure 5.1. TEM micrographs of (a) lower bainite and (b) tempered martensite of JIS SK5 steel [37]

In the bainitic microstructure of 60SiMn5 (Figure 4.24 (b) and (d)) the bainitic ferrite sheaves on austenite phase matrix are clearly seen. When the SEM images of bainitic microstructures of 55Cr3 and 60SiMn5 are compared, the carbide precipitates are clearly visible both in ferrite sheaves and in austenite matrix of steel 55Cr3. However, there is no carbide precipitation in 60SiMn5 lower bainite as illustrated in Figure 4.24 (a) and (c). The difference in the microstructures is due to the presence of Si in 60SiMn5 which prevents carbide precipitation and hence carbon is rejected into the austenite. As a consequence, the M_s temperature of austenite drops and the austenite between the sheaves cannot transform to martensite upon cooling. According to Bhadeshia and Caballero, the preservation of retained austenite films between the bainite sheaves improves the toughness by crack propagation resistance [16,44,45].

In SEM image of 60SiMn5 carbide-free lower bainite, there are islands in the microstructures which can be considered as either martensite or retained austenite (Figure 4.24 (d)). However, these islands are generally called M/A (Martensite/austenite) and does not contribute to toughness.

5.2. Comparison of Mechanical Properties of 55Cr3 and 60SiMn5 Samples

In this study, it was aimed to compare the mechanical behavior of tempered martensite with bainite in 55Cr3. All of the mechanical test results of 55Cr3 were summarized in Table 4.6. Firstly, the hardness of as-quenched martensite was measured and seen that is was 770HV. Such a high hardness means that the austenite fully transformed into martensite. The martensitic samples that tempered at 220°C for 5 hours, and 450°C, 500°C, 550°C for 1.5 hours have hardness values of 653HV, 480HV, 435HV, and 396HV, respectively. The hardness values decreased as the temperature increased and as gathered from the literature there is a similar study for 55Cr3 done by Htun et.al., They used the same tempering temperatures at various tempering times from 1 hour to 3 hours and air cooled the samples. The hardness values in their study for 55Cr3 steel that tempered at 450°C, 500°C, 550°C for 1 hour are 448HV, 424HV, and 406HV which correspond to the results in this study [41]. The reason for the decrease in

hardness is because of the softening effect of high temperature. This softening effect occurs by coarsening of carbides and decrease in the tetragonality of martensite [38].

In the case of bainitic microstructures, the presence of martensite in bainite effect the overall hardness. The sample held at 270°C for 8 minutes has a hardness value of 635HV. This result is higher than that of 100% lower bainitic microstructures since the sample contains fresh martensite as it was quenched to room temperature.

The lower bainitic (270°C, 80min) and tempered lower bainitic (270°C, 3hr) microstructures of 55Cr3 have the hardness values of 583HV and 570HV, respectively. As it can be seen from the results, tempering does not cause softening in lower bainitic sample. Woodhead et.al. stated that since rather than residing in a solid solution, the carbon precipitates in bainitic ferrite sheaves and these carbide precipitates are coarser when compared with tempered martensite [39]. Hence, in contrast to martensite, carbides already exist within the bainite sheaves and their size does not change at isothermal transformation temperatures. However, the carbon in martensite is supersaturated and precipitate with a fast rate upon tempering. Therefore, it can be stated that the strengthening mechanism in bainite and martensite is different. In bainitic microstructure, the strength depends on the fine grain size, i.e. the thickness of bainite sheaves, whereas in martensite the solid solution of carbon results in high strength and consequently high hardness [40].

From the hardness test results, the lower bainitic microstructure of 55Cr3 is especially compared with “220°C, 5hr” tempered martensite sample for other mechanical properties, since they have close hardness values among all other tempered martensitic samples, i.e., 583HV for lower bainite and 653HV for tempered martensite.

When compared the hardness values of lower bainite of 55Cr3 and carbide-free lower bainite of 60SiMn5, the carbide-free lower bainite of 60SiMn5 was expected to have much higher hardness since its carbon content is nearly 0,03% higher than 55Cr3. However, Cr is frequently included in bainitic steels to extend their hardenability so that a slower cooling rate can be utilized to prevent high temperature ferrite formation

and bainite can be achieved more easily. Yet, this does not mean that Cr boosts bainitic transformation, it inhibits ferrite formation and by so increases the hardenability. Although it has been studied that Cr decreases the lower bainite transformation kinetics in a continuous cooling, its effect on lower bainite formation in isothermal transformation processes is still a matter of concern. In the study of Zhou et.al., it was seen that Cr addition decreases the kinetics of bainitic transformation at lower temperatures. When the lower bainitic transformation temperature is 400°C for a Cr-added and a Cr-free steels, and it was seen that the amount and the morphology of bainite showed no reasonable change (Figure 5.2). On the other hand, when the temperature increased to 430°C and 450°C, it was seen that bainite amount decreased and martensite amount increased in Cr-added steel. [15-21].

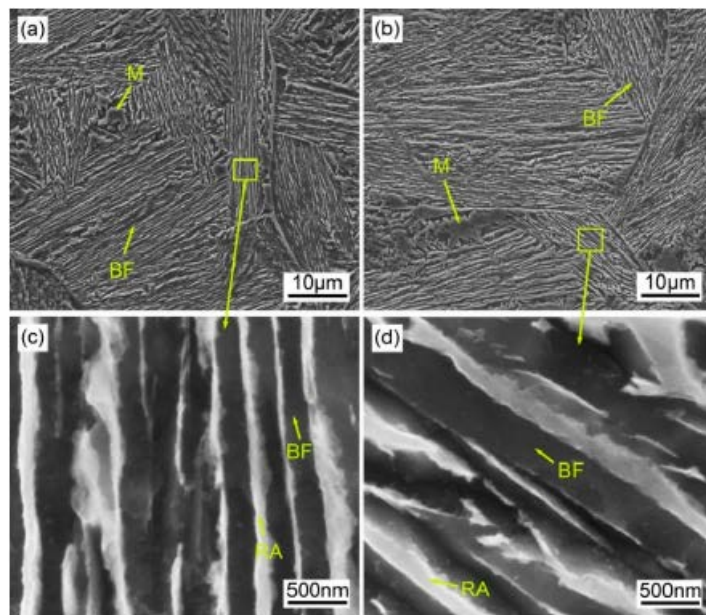


Figure 5.2. Cr-free and Cr-added steels austempered at 400°C; (a,c) Cr-free steel; (b,d) Cr-added steel. M, martensite; BF, bainitic ferrite; RA, retained austenite.[15]

When looking at tensile test experiments, the “220°C, 5hr”, “450°C, 1.5hr”, “500°C, 1.5hr” and “550°C,1.5hr” tempered martensitic samples resulted in lower tensile properties than expected. As it was summarized in Table 4.6, the “220°C, 5hr” sample

was ruptured prematurely with no strain. The “450°C, 1.5hr”, “500°C, 1.5hr” and “550°C,1.5 hr” samples have yield strength values of 1222MPa, 992 MPa, and 986 MPa, respectively. Their UTS values are 1269MPa, 1018MPa, and 1011MPa, respectively. In their study, Htun et. al. achieved yield strength values of 1400MPa, 1100MPa, 1000MPa and UTS values of 1600MPa, 1300MPa, 1100MPa for the samples tempered at 450°C, 500°C, 550°C for 1 hour, respectively. By taking into consideration that the tempering time in the study of Htun et.al. is half hour shorter than that used in this study, the yield strength and UTS values are close to each other.

However, the strain values of the tempered samples were far lower than expected. While the “450°C, 1.5hr”, “500°C, 1.5hr” and “550°C,1.5 hr” samples in this study yielded 0,2%, 0,9% 0,9%, 1,4% strain values, Htun et. al. obtained strains from 5% to 10% for 1-hour of tempering at 450°C, 500°C, 550°C. It is quite interesting that although yield strength and ultimate tensile strength values are similar, strain values of the samples in this study are very low. All the tempered specimens behaved brittle. Therefore, although oil, as a quench media, may create more residual stresses and brittleness when compared to air cool, the strain values that cannot go beyond 1,4% (550°C, 1.5hr) still need clarification.

On the other hand, the bainitic samples yielded very good tensile properties. The lower bainitic “270°C, 80min” and “220°C, 3hr” samples have yield strengths of 1645MPa and 1638MPa and ultimate tensile strengths of 1978MPa and 1961MPa respectively. Their elongation values are 9,7% and 10,5%. From this point of view, it is obvious that the lower bainitic samples have far greater tensile properties than that of tempered martensitic samples. They are especially superior to that of “220°C, 5hr” tempered martensite sample, which have the closest hardness to lower bainite.

It might be more appropriate to compare the sample “270°C, 8min” sample with the “240°C, 5hr” sample. The former has fresh martensite and lower bainite in its microstructure and the latter has tempered martensite and lower bainite. From Table 4.6, it is seen that yield strength values of “270°C, 8min” and “240°C, 5hr” samples

are 1187MPa and 1760MPa. Moreover, their UTS values are 1263MPa and 1780MPa, respectively. It was an expected result that the “270°C, 8min” sample has low strain and strength values since it has fresh martensite in it. However, although “240°C, 5hr” has superior strength values, it was unexpected to have low strain value. This may possibly be due to being 240°C is not enough for tempering the martensite sufficiently.

When the fracture surfaces of tensile test specimens are considered, “270°C, 80min” sample contains more dimples and exhibit a ductile fracture. However, other samples’ fracture surfaces mostly comprise of cleavage-type of fracture. The more ductile behavior of “270°C, 80min” sample was already understood looked at its higher strain value among others in Table 4.6.

The Charpy impact test results showed, the “450°C, 1.5hr”, “500°C, 1.5hr” and “550°C, 1.5hr” tempered martensite samples had 20.7J, 21.7J, and 21J impact energies. The “220°C, 5hr” sample has very low impact energy (3.3J) which ensures that this sample was in under-tempered condition.

The lower bainitic “270°C, 80min” and “270°C, 3hr” samples have 12.7J and 11.7J of impact energies.

The “270°C, 8min” and “240°C, 5hr” samples have impact energies of 2.3J and 8.3J, respectively. Fresh martensite in “270°C, 8min” caused lower toughness value while tempering the martensite showed increasing effect on the toughness in “240°C, 5hr” sample.

When looking at their fracture surfaces after Charpy impact tests, tempered martensitic samples mostly consists of dimples (Figure 4.26 and Figure 4.27), while lower bainitic and bainitic-martensitic mixed samples showed quasi-cleavage type of fracture (Figure 4.34 and Figure 4.36.). The reason for lower bainite to have lower toughness than that of tempered martensitic samples can be the carbide precipitates acting as stress concentrators [43].

Within the comparison of different variations of lower bainitic and tempered martensitic samples of 55Cr3 steel, the fully bainitic “270°C, 80min” sample has the best tensile properties in terms of yield strength, ultimate tensile strength and strain, in addition to its good toughness property. In addition to its superior properties, the elimination of subsequent heat treatment like tempering is an important advantage of lower bainite.

If the lower bainite of 55Cr3 is compared with the carbide-free lower bainite of 60SiMn5, their hardness values are 583HV and 600HV, respectively. By looking at these values, they are considered to have the same hardnesses. The yield strength values are 1645MPa and 1781MPa; moreover, the ultimate tensile strength values are 1984MPa and 2107MPa respectively. The UTS of carbide-free lower bainite of 60SiMn5 has approximately 150MPa greater than the lower bainite of 55Cr3 in both strength values. In addition, as it can be seen from Figure 5.3, the lower bainite of 55Cr3 is much more ductile as its elongation is almost more than twice the value for carbide-free lower bainite of 60SiMn5.

A spring material is expected to have a good resilience property so that it can response to the loads applied to that as much elastically as possible. The resilience property is determined by calculating the area under tensile stress – tensile strain curve in the elastic region. As it can be seen from Figure 5.3 the elastic region for carbide-free lower bainite of 60SiMn5 is determined by offset method and it is observed that the area under tensile stress – tensile strain curve in the elastic region, in other words, the resilience property value of lower bainite of 55Cr3 is higher than that for carbide-free lower bainite of 60SiMn5.

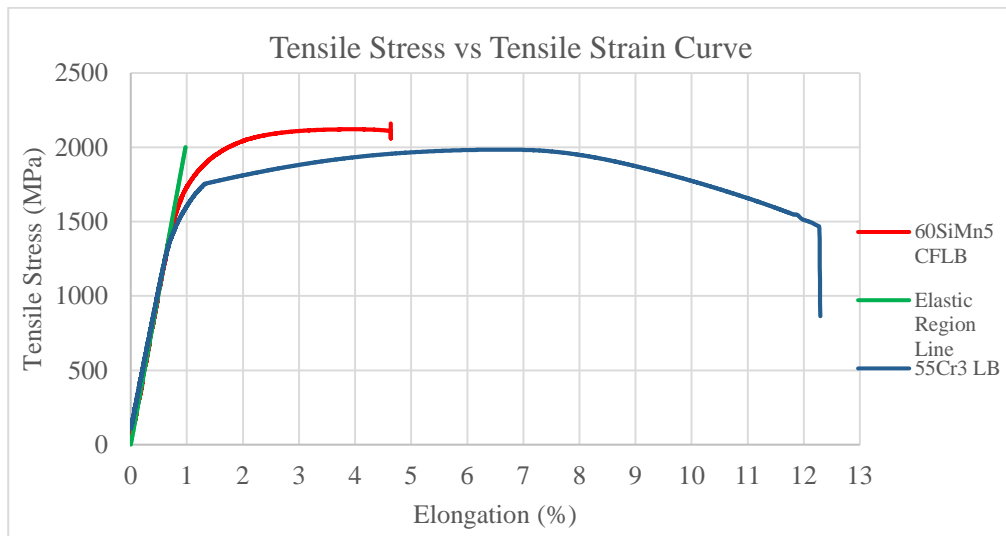


Figure 5.3. Comparison of the tensile properties of 55Cr3 LB and 60SiMn5 CFLB

For spring applications, the steel is also expected to have good toughness and strength proportion. Therefore, samples containing lower bainite were compared in terms of their Charpy impact energies and tensile strengths. It is seen from Figure 5.4 that the best proportion is caught with the 100% lower bainitic sample of 55Cr3 steel. The tempered lower bainite of 55Cr3 has also a good proportion, while carbide-free lower bainite of 60SiMn5 has less value than both of them.

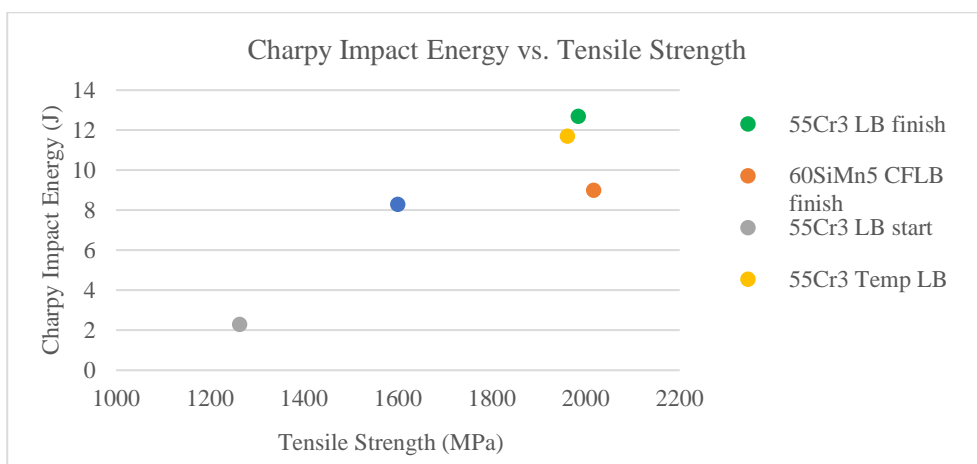


Figure 5.4. Charpy Impact Energy vs. Tensile Strength of lower bainitic microstructures of 55Cr3 and 60SiMn5

Lower bainitic samples of both 55Cr3 and 60SiMn5 have good toughness values; yet, still they are not superior than tempered martensite in terms of toughness. This can be because of existence of the coarse M/A islands in lower bainite which can act as stress concentration points [42].

CHAPTER 6

CONCLUSION

In this study, 55Cr3 and 60SiMn5 steels were used to obtain lower bainitic microstructures. Firstly, martensitic microstructures that tempered at various temperature and time periods were compared with lower bainitic microstructures of 55Cr3. Then the lower bainitic microstructure of 55Cr3 and carbide-free lower bainitic microstructure of 60SiMn5 were compared. The comparisons were based on both microstructural examinations and mechanical properties. From the results of this study, below conclusions can be deduced:

1. The lower bainitic microstructure in 55Cr3 steel was obtained by isothermal transformation at 270°C for 80min. On the other hand, for 60SiMn5 steel 5,5hrs is needed at 250°C to obtain fully bainitic microstructure.
2. The 100% bainitic structures of 55Cr3 and 60SiMn5 yielded similar hardness values in the range 580HV-600HV. On the other hand, the hardness of quenched and tempered specimens of both steels were lower than their bainitic counterparts by yielding a hardness interval of 395HV-480HV if tempered in the range 450C-550C. Only the hardness of quenched 55Cr3 specimen was comparable to hardnesses of bainitic specimens if tempered at 250C for 5hrs by yielding 650HV.
3. The 100% bainitic structures of both 55Cr3 and 60SiMn5 steels yielded very high strength values exceeding 1900MPa. At this strength level the elongations of specimens were over 6%. On the other hand, the tensile strength of the quenched and tempered specimens was lower than 1600 MPa with no ductility.
4. The Charpy impact values of the bainitic samples were slightly lower than that of quenched and tempered specimens which is related to the lower hardness values of the martensitic specimens.

5. As far as the 55Cr3 specimens consisting of martensite-bainite phase mixture are concerned: The specimens isothermally treated after quenched to a temperature between Ms and Mf always yielded higher strength and toughness values with respect to the specimens isothermally treated for a short period of time just above Ms.
6. There was no considerable difference between the mechanical properties of bainitic 55Cr3 and 60SiMn5 specimens, although the bainite in 60SiMn5 steel was free of carbide precipitation.

REFERENCES

- [1] H. K. D. H. Bhadeshia, *Bainite in Steels*, 2nd ed. London: IOM Communications Ltd, 2001.
- [2] E. C. Bain, *Functions of alloying elements in steel*, 4th ed. American Society for Metals, 1939.
- [3] J. C., J. L., & J. W. (2012). Modelling phase transformations in hot stamping and cold die quenching of steels. In *Microstructure Evolution in Metal Forming Processes* (Woodhead Publishing Series, pp. 210-235).
- [4] Smallman, R. E., & Ngan, A. H. (2014). *Modern Physical Metallurgy* (8th ed.). Oxford, UK: Elsevier.
- [5] Krauss, G. (1999, December 15). Martensite in steel: Strength and structure. *Materials Science and Engineering: A*, 273(275), 40-57.
- [6] Krauss, G. (2012). Tempering of martensite in carbon steels. *Phase Transformations in Steels*, 2, 126-150.
- [7] Bhadeshia, H., & Honeycombe, R. (2017). Chapter 9 - Tempering of Martensite. In *Steels: Microstructure and Properties* (4th ed., pp. 237-270). Elsevier.
- [8] H.K.D.H. Bhadeshia, A. Strang, D.J. Gooch, Ferritic power plant steels: remanent life assessment and the approach to equilibrium, *International Materials Reviews* 43 (1998) 45–69.
- [9] Bailey, N. (1994). Service Problems. *Weldability of Ferritic Steels*, 210-223.
- [10] Berns, H., & Theisen, W. (2008). *Ferrous Materials: Steel and Cast Iron*. Bochum: Springer-Verlag, 45-48.
- [11] Hillert, M. (1994, September). Diffusion in Growth of Bainite. *Materials Science and Engineering: A*, 25(9), 1957-1966.
- [12] Moore, D. J., Rouns, T. N., & Rundman, K. B. (1985, June). The effect of heat treatment, mechanical deformation, and alloying element additions on the rate of bainite formation in austempered ductile irons. *Journal of Heat Treating*, 4(1), 7-24.
- [13] Soliman, M., & Palkowski, H. (2016). Development of the low temperature bainite. *Archives of Civil and Mechanical Engineering*.
- [14] Ramesh, G., & Prabhu, N. K. (2011, April). Review of thermo-physical properties, wetting and heat transfer characteristics of nanofluids and their applicability in industrial quench heat treatment. *Nanoscale Research Letters*, 6(334).
- [15] Zhou, M., Xu, G., J., Hu, H., & Yuan, Q. (2017, July 10). Bainitic Transformation and Properties of Low Carbon Carbide-Free Bainitic Steels with Cr Addition. *Metals*, 7(263).
- [16] Caballero, F.G.; Bhadeshia, H.K.D.H.; Mawella, K.J.A.; Jones, D.G.; Brown, P. Design of novel high strength bainitic steels. Part 1. *Mater. Sci. Technol.* 2001, 17, 512–516.

- [17] Caballero, F.G.; Bhadeshia, H.K.D.H. Very strong bainite. *Curr. Opin. Solid State Mater.* 2004, 8, 251–257.
- [18] Caballero, F.G.; Santofimia, M.J.; Garcia-Mateo, C.; Chao, J.; de Garcia Andres, C. Theoretical design and advanced microstructure in super high strength steels. *Mater. Des.* 2009, 30, 2077–2083.
- [19] Hasan, H.S.; Peet, M.J.; Avettand-Fènoël, M.-N.; Bhadeshia, H.K.D.H. Effect of tempering
- [20] Bracke, L.; Xu, W. Effect of the Cr content and coiling temperature on the properties of hot rolled high strength lower bainitic steel. *ISIJ Int.* 2015, 55, 2206–2211.
- [21] Bhadeshia, H., & Honeycombe, R. (2017). Tempering of Martensite. In *Steels: Microstructure and Properties*.
- [22] Bhadeshia, H. K. D. H. (2014). Physical Metallurgy of Steels. In *Physical Metallurgy: Fifth Edition* (Fifth Edit, Vol. 1).
- [23] García-Mateo, C., Caballero, F. G., & Bhadeshia, H. K. D. H. (2009). Mechanical Properties of Low-Temperature Bainite. *Materials Science Forum*, 500–501(November), 495–502.
- [24] Min Shan, H., Si Thu, K., & Kay Thi, L. (2008). Effect of Heat Treatment on Microstructures and Mechanical Properties of Spring Steel. *Journal of Metals, Materials and Minerals*, 18(2), 191–197.
- [25] Tian, J., Xu, G., Zhou, M., Hu, H., & Wan, X. (2017). The Effects of Cr and Al Addition on Transformation and Properties in Low-Carbon Bainitic Steels. *Metals*, 7(2), 40.
- [26] Krauss, G. (2014). Quench and Tempered Martensitic Steels: Microstructures and Performance. *Comprehensive Materials Processing*, 12, 363–378.
- [27] B.P.J. Sandvik, H.P. Nevalainen. (1981). Structure–property relationships in commercial low-alloy bainitic–austenitic steel with high strength, ductility, and toughness. *Materials Science and Technology*, 8, 213–220.
- [28] Soliman, M., Palkowski, H. (2016). Development of the low temperature bainite. *Archives of Civil and Mechanical Engineering*, 16(3), 403–412.
- [29] Rhana, Ed. R., Singh S.B. (2017). *Automotive Steels; Design, Metallurgy, Processing and Applications*. Woodhead Publishing (Elsevier).
- [30] Sikka, V.K., Klueh, R.L., Maziasz, P.J., Babu, S., Santella, M.L., Jawad, M.H. (2004). Mechanical properties of new grades of Fe–3Cr–W alloys, *American Society of Mechanical Engineers Pressure Vessel and Piping Division*, 476, 97–106.
- [31] Abe, F. (2004). Bainitic and martensitic creep-resistant steels. *Current Opinion in Solid State and Materials Science*, 8(3–4), 305–311.
- [32] Matlock, D. K., Krauss, G., & Speer, J. G. (2001). Microstructures and properties of direct-cooled microalloy forging steels. *Journal of Materials Processing Technology*, 117(3), 324–328.

- [33] Ceschini, L., Marconi, A., Martini, C., Morri, A., & Di Schino, A. (2013). Tensile and impact behaviour of a microalloyed medium carbon steel: Effect of the cooling condition and corresponding microstructure. *Materials and Design*, 45(January 2015), 171–178.
- [34] Hairer, F., Karellova, A., Kremaszky, C., Werner, E. et. al. (2009). Influence of Heat Treatment on the Microstructure and Hardness of a Low Alloyed Complex Phase Steel. *Proceedings from the Materials Science & Technology Conference*. (October, 2009), 78-83.
- [35] Demeri, M.Y. (2013). Advanced High Strength Steels: Science, Technology and Applications. *ASM International*.
- [36] Nagode, A., Resnik, A., Vertnik, R., Bizjak, M., Kosec, B., Gojić, M., Zorc, B. (2017). The development of a banded microstructure in S355J2 steel bar. *Kovove Materialy*, 55(1), 51–56.
- [37] Tu, M., Hsu, C., Wang, W., & Hsu, Y. (2008). *Comparison of microstructure and mechanical behavior of lower bainite and tempered martensite in JIS SK5 steel*. 107, 418–425.
- [38] Ezechidelu, J. C., Enibe, S. O., Obikwelu, D. O., Nnamchi, P. S., & Obayi, C. S. (2016). Effect of Heat Treatment on the Microstructure and Mechanical Properties of a Welded AISI 410 Martensitic Stainless Steel. *Iarjset*, 3(4), 6–12.
- [39] Woodhead, J. H., Quarrell, A. G., 1965. Role of carbides in low alloy creep resisting Steels. *Journal of the Iron and Steel Institute* 203, 605–620.
- [40] Irvine, K.J., Pickering, F.B., 1957. Low carbon bainitic steels. *Journal of the Iron and Steel Institute* 187, 292-309.
- [41] Min Shan, H., Si Thu, K., & Kay Thi, L. (2008). Effect of Heat Treatment on Microstructures and Mechanical Properties of Spring Steel. *Journal of Metals, Materials and Minerals*, 18(2), 191–197.
- [42] Caballero, F.G., Roelofs, H., Hasler, St., Capdevila, C. (1966). Influence of bainite morphology on impact toughness of continuously cooled cementite-free bainitic steels. *The British Journal of Psychiatry*, 112(483), 211–212.
- [43] Johnson, D. R., & Becker, W. T. (1993). Toughness of tempered upper and lower bainitic microstructures in a 4150 steel. *Journal of Materials Engineering and Performance*, 2(2), 255–263.
- [44] F.G. Caballero, Bhadeshia HKDH, Mawella KJA, Jones DG, Brown P. Design of novel high strength bainitic steels. Part 2. *Mater Sci Technol* 2001;17:517–22.
- [45] F.G. Caballero, Santofimia MJ, Capdevila C, García-Mateo C, García de Andrés C. Design of advanced bainitic steels by optimization of TTT diagrams and To curves. *ISIJ Int* 2006;46:1479–88.

CURRICULUM VITAE

PERSONAL INFORMATION

Surname, Name : BAKIR, SİMGE
Nationality : Turkish (TC)
Date and Place of Birth : 07 July 1989, Ankara
Phone : +90 506 562 97 79
E-mail : e174507@metu.edu.tr

EDUCATION

Degree	Institution	Year of Graduation
BS	METU Met. And Mat. Engineering	2015
High School	Kaya Bayazıtöđlu Lisesi, Ankara	2007

WORK EXPERIENCE

Year	Place	Enrollment
2018-Present	GE Aviation	Special Processes Engineer
2016-2018	TAI	Manufacturing Engineer
2015-2016	Türk Traktör	Test Engineer

FOREIGN LANGUAGES

Advanced English, Basic German

HOBBIES

Running, Tennis, Scuba Diving, Volleyball, Sewing, Travelling, Photography